Popular Summary

Since first light in early 2000, operational global quantitative retrievals of aerosol properties over land have been made from MODIS observed spectral reflectance. These aerosol products have been used for dozens of applications, including some not even imagined before launch. We have been continuously evaluating and validating the algorithm and products, and have noted opportunities for their improvement. In early 2006, we replaced the original algorithm. This new algorithm (known as Version 5.2 or V5.2) performs a simultaneous inversion of two visible channels (0.47 and 0.66 μm), plus a shortwave-IR (2.12 μm) channel, thus improving sensitivity to the scattering of coarse aerosols (> 1 μm in radius) such as dust. Also, we have improved the assumptions related to surface reflectance, aerosol optical properties, and radiative transfer calculations. Inversion of the three channels yields three nearly independent parameters, the aerosol optical depth (τ) at 0.55 μm, the non-dust or fine weighting (η) and the surface reflectance at 2.12 μm. Retrievals of small magnitude negative τ values (down to -0.05) are now considered valid, thus normalizing the statistics of τ in near zero τ conditions. On a "test-bed" of 6300 granules from both *Terra* and *Aqua* satellite platforms, the products from V5.2 show marked improvement over those from the previous versions. Compared with surface based sunphotometer (AERONET) observations, regression of MODIS τ (at 0.55 μm) has an equation of: $y = 1.01x + 0.03$, $R = 0.90$. Mean τ for the test-bed is reduced from 0.28 to 0.21, which is more in line with estimates from transport models. We also added some new products for V5.2, including "fine aerosol τ" and spectral surface reflectance. The new algorithm began operational production of "Collection 005" in April 2006, and is expected to finish re-processing the entire MODIS mission by the end of 2006.

A new algorithm for retrieving aerosol properties over land from MODIS spectral reflectance

Robert C. Levy[1,2,3], Lorraine A. Remer[2], Shana Mattoo[1,2], Eric F. Vermote[4] and Yoram J. Kaufman[2]

[1] Science Systems and Applications Inc., Lanham MD

[2] Laboratory for Atmospheres, NASA/Goddard Space Flight Center, Greenbelt MD

[3] Department of Atmospheric and Oceanic Science, University of Maryland, College Park, MD

[4] Department of Geography, University of Maryland, College Park, MD

Corresponding author's address: Mr. Robert Levy   301-614-6123 (voice)
                                   SSAI   301-614-6307 (fax)
                                   Code 613.2
                                   NASA/Goddard Space Flight Center
                                   Greenbelt MD 20771
                                   Email: levy@climate.gsfc.nasa.gov

A new algorithm for retrieving aerosol properties over land from MODIS spectral reflectance

Robert C. Levy[1,2,3], Lorraine A. Remer[2], Shana Mattoo[1,2], Eric F. Vermote[4] and Yoram J. Kaufman[2]

[1] Science Systems and Applications Inc., Lanham MD

[2] Laboratory for Atmospheres, NASA/Goddard Space Flight Center, Greenbelt MD

[3] Department of Atmospheric and Oceanic Science, University of Maryland, College Park, MD

[4] Department of Geography, University of Maryland, College Park, MD

Corresponding author's address: Mr. Robert Levy   301-614-6123 (voice)
                                    SSAI   301-614-6307 (fax)
                                    Code 613.2
                                    NASA/Goddard Space Flight Center
                                    Greenbelt MD 20771
                                    Email: levy@climate.gsfc.nasa.gov

A new algorithm for retrieving aerosol properties over land from MODIS spectral reflectance

Robert C. Levy, Lorraine A. Remer, Shana Mattoo, Eric Vermote, Yoram J. Kaufman

Since first light in early 2000, operational global quantitative retrievals of aerosol properties over land have been made from MODIS observed spectral reflectance. These products have been continuously evaluated and validated, and opportunities for improvements have been noted. We have replaced the original algorithm by improving surface reflectance assumptions, the aerosol model optical properties and the radiative transfer code used to create the lookup tables. The new algorithm (known as Version 5.2 or V5.2) performs a simultaneous inversion of two visible (0.47 and 0.66 μm) and one shortwave-IR (2.12 μm) channel, making use of the coarse aerosol information content contained in the 2.12 μm channel. Inversion of the three channels yields three nearly independent parameters, the aerosol optical depth (τ) at 0.55 μm, the non-dust or fine weighting (η) and the surface reflectance at 2.12 μm. Finally, retrievals of small magnitude negative τ values (down to -0.05) are considered valid, thus normalizing the statistics of τ in near zero τ conditions. On a 'test bed' of 6300 granules from Terra and Aqua, the products from V5.2 show marked improvement over those from the previous versions, including much improved retrievals of τ, where the MODIS/AERONET τ (at 0.55 μm) regression has an equation of: y = 1.01x + 0.03, R = 0.90. Mean τ for the test bed is reduced from 0.28 to 0.21.

1. Introduction

Aerosols are major players in Earth's climate, radiation budget, cloud processes and air quality, and increasingly sophisticated and accurate remote sensing techniques have been introduced to understand aerosols and their effects. Especially for aerosols over land, the first operational global satellite dataset has been provided by the Moderate Imaging Spectrometer (MODIS). Since MODIS' launch aboard *Terra* (in late 1999) and aboard *Aqua* (in early 2002), the use of the MODIS aerosol products has grown exponentially. Since launch, MODIS data and specifically aerosol data have been used for dozens of applications and in hundreds of publications. Not only have MODIS aerosol products been used to answer (intended) scientific questions about radiation and climate (e.g. IPCC, 2001; Yu et al., 2006), they are being used for applications not previously intended. One example is using MODIS to monitor surface air quality for health (e.g. Chu et al., 2003; Al-Saadi et al., 2005).

The operational algorithm over land has been using MODIS reflectance data in three channels (0.47, 0.66 and 2.12 μm; channels 3, 1 and 7) to retrieve total spectral 'aerosol optical depth' (AOD or τ) and 'Fine aerosol Weighting' (FW or η), reported at 0.55 μm. Since launch, the aerosol products have been monitored for quality, and the algorithm has been continuously updated. Details of a previous version (V4.2) and the products created for 'Collection 004' (C004) has been described in Remer et al., (2005). The last update to the algorithm was known as 'V5.1', but it never became operational.

In order to be applied in both climate and air pollution applications, MODIS aerosol retrievals must meet certain expected accuracy (Kaufman et al. 1997a). MODIS should be able to retrieve τ to within expected errors, specifically:

$$\Delta\tau = \pm 0.05 \pm 0.15\tau \qquad\qquad (1)$$

(Remer et al., 2005). To this end, a number of papers have attempted to 'validate' the retrieved properties of C004 and before, by comparing MODIS derived values to standard (ground truth) aerosol measurements, using the co-location theory of Ichoku et

3

al., (2002). Ground based sunphotometers, especially from the Aerosol Robotic NETwork (AERONET – (Holben et al., 1998)), have provided the bulk of the comparison data (e.g. Chu et al., 2002; Levy et al., 2005; Remer et al., 2005; Ichoku et al. 2005). Most of these validation studies have shown that although MODIS generally derives τ within the expected error, MODIS tends to over-estimate τ for small τ and underestimate for high τ (Chu et al, 2002; Remer et al. 2005; Levy et al. 2005). In fact, at 0.55 μm, the consensus is a MODIS/AERONET τ regression of approximately

$$\tau_{MODIS} = 0.1 + 0.9\,\tau_{AERONET}. \tag{2}$$

Why is the regression not one to one? The algorithm made a number of assumptions as to the aerosol optical properties, surface reflectance, MODIS channel central wavelengths, Rayleigh (molecular) optical depth, radiative transfer, transparency of 2.12 μm channel, and retrieval philosophy/logic. This paper introduces a new aerosol retrieval algorithm, known as 'V5.2' that analyzes the validity of each assumption in the C004 algorithm. Section 2 introduces the C004 MODIS products and AERONET data used in this study. Section 3 summarizes the new aerosol models and look-up table described by Levy et al., (2006). The surface reflectance properties are discussed in Section 4. Section 5 introduces a new retrieval philosophy, and section 6 discusses the products that will be Collection 5 (C005). Finally, we show some provisional validation of V5.2 in Section 7.

2. The MODIS C-004 and AERONET L2A datasets

For this work, we made extensive use of both MODIS and AERONET data products. Aerosol products have been derived from Terra reflectance observations since 2000 and since 2002 from Aqua. As of early 2005, most MODIS observations ('Level 1') through 2004 had been processed or re-processed into 'Level 2 products' (L2) using consistent retrieval algorithms. This collection of products is known as 'Collection 4' or 'C004'. At some sites, AERONET has been reporting since 1993, and as of early 2005, most of the AERONET data have been re-processed and quality assured by the AERONET team. These products are also known as 'Level 2', but to differentiate them from the MODIS products, we denote the AERONET products as 'L2A'.

The MODIS instruments aboard Terra and Aqua both measure spectral radiance in 36 channels, in resolutions between 250 m and 1 km (at nadir). In polar-orbit about 700 km above the earth, MODIS views a swath about 2300 km, resulting in near daily global coverage of Earth's land/ocean/atmosphere system. The swath is broken into five-minute 'granules', each about 2030 km long. The aerosol algorithm over land makes use of gas-absorption corrected spectral solar reflectance measurements (in visible through the IR bands) to perform cloud masking and pixel selection, and then retrieve aerosol optical depth (AOD or τ) and fine-dominated aerosol fraction (known as 'fine weighting', FW or η) at 10 km resolution (at nadir).

The basic concepts of the land algorithm was introduced by Kaufman et al., (1997a) and updated by Remer et al., (2005) to describe the products of C004. From pre-launch through C004, the algorithm has gone through a series of updates, detailed at http://modis-atmos.gsfc.nasa.gov/MOD04_L2/history. The theory of the MODIS over-land algorithm is as follows. The upward spectral 'reflectance' (normalized solar radiance) at the top of the atmosphere (TOA) is a function of successive orders of radiation interactions within the coupled surface-atmosphere system. The TOA angular (θ_0, θ, ϕ = solar zenith, view zenith and relative azimuth angles) spectral reflectance ($\rho_\lambda(\theta_0, \theta, \phi)$) at a wavelength λ results from: scattering of radiation within the atmosphere without interaction with the surface (known as the 'atmospheric path reflectance'), the reflection of radiation off the surface that is directly transmitted to the TOA (the 'surface function'), and the reflection of radiation from outside the sensor's field of view (the 'environment function'). The environment function is neglected so that to a good approximation:

$$\rho_\lambda^*(\theta_0,\theta,\phi) = \rho_\lambda^a(\theta_0,\theta,\phi) + \frac{F_\lambda(\theta_0)T_\lambda(\theta)\rho_\lambda^s(\theta_0,\theta,\phi)}{1 - s_\lambda\rho_\lambda^s(\theta_0,\theta,\phi)} \qquad (3)$$

where $F_{d\lambda}$ is the 'normalized downward flux' for zero surface reflectance, T_λ represents 'upward total transmission' into the satellite field of view, s_λ is the 'atmospheric backscattering ratio', and ρ_λ^s is the angular 'surface reflectance'. Except for the surface reflectance, each term on the right hand side of Equation 3 is a function of the aerosol type and loading (τ). Assuming that a small set of aerosol types and loadings can describe the range of global aerosol, we have created a lookup table that contains pre-computed

5

simulations of these aerosol conditions. The goal of the algorithm is to use the lookup table to determine the conditions that best mimic the MODIS-observed spectral reflectance $\rho^m{}_\lambda$, and retrieve the associated aerosol properties (including τ and η). The difficulty lies in making the most appropriate assumptions about both the surface and atmospheric contributions.

The sunphotometers of the Aerosol Robotic NETwork (AERONET) provide a comprehensive data set of aerosol properties. These include direct 'sun' measurements of spectral τ in four or more wavelengths (to include 0.44, 0.67, 0.87 and 1.02 μm), and indirect 'sky' measurements that lead to estimates of aerosol optical properties and aerosol size distributions (Holben et al., 1998). These data go through rigorous calibration and cloud screening processes, resulting in the L2A products. The AERONET direct sun measurements are made approximately every 15 minutes during mid-day and more often during sunrise and sunset. In addition to spectral τ, AERONET also provides estimates of columnar water vapor w (precipitable water in units of [cm]). O'Neill et al. (2003) developed a method for estimating η from the direct sun measurements of spectral τ. The AERONET sky radiance measurements are made less often (about once per hour), and are inverted simultaneously either assuming spherical aerosol particles (Dubovik and King, 2000) and/or spheroid particles (Dubovik et al., 2002; Dubovik et al., 2006). Under either particle assumption, the fundamental derived parameters include spectral τ, spectral complex refractive index, the volume distribution as a function of 22 radius size bins (dV/dlnR), and fitting error to the radiance measurements. Additional parameters are then calculated that include Ångstrom exponents, properties of two (fine and coarse mode) lognormal aerosol distributions, spectral single scattering albedo (SSA or ω_0) and asymmetry parameter (g) of the lognormal modes.

Although the actual products provided by MODIS and AERONET are not necessarily physically identical, in many cases they are comparable. For example, MODIS retrieves τ at 0.55 μm, whereas AERONET retrieves at 0.44 and 0.67 μm, and some instruments also measure at 0.50 μm. However, fitting a quadratic equation through the logarithms of both τ and wavelength, AERONET τ can be interpolated to 0.55 μm (Eck et al., 1999). Comparison of η is trickier. Over land, MODIS considers η to be the contribution of the fine-dominated model (the non-dust model) to the total τ, the

AERONET sky retrievals designate η to be the volume contribution from aerosol below a radius of 0.6 μm, whereas the O'Neill method separates fine and coarse aerosol by spectral behavior. Practically, however, the definitions of η are similar enough so that they should be correlated (Kleidman et al., 2005, Anderson et al., 2005, Chu et al. 2005).

Over 15,000 pairs of MODIS and AERONET 'sun' data, at over 200 global sites, have been co-located in time via the technique of Ichoku et al., (2002). A valid MODIS/AERONET match is considered when there at least five (out of a possible 25) MODIS retrievals (10 km x 10 km resolution) within the box, and at least two (out of a possible five) AERONET observations within the hour. This co-located data set was used for a number of applications described in this document, including studies of surface reflectance, and validation of MODIS products.

3. New aerosol lookup tables

A number of studies (e.g. Chu et al., 2002, Remer et al., 2005, Levy et al., 2005) have demonstrated that MODIS/AERONET regression of τ over land results in slope less than one; meaning that MODIS tends to under-estimate optical depth, especially as the optical depth increases. Ichoku et al., (2003) and Levy et al., (2005) found that updating the assumed aerosol properties in Southern Africa and the U.S. East Coast, respectively, improved the retrieval in those regions. Results from studies such as these led Levy et al., (2006) to consider deriving new aerosol optical models for V5.2, using over 136,000 AERONET sky retrievals.

Levy et al., (2006) performed a cluster analysis of spherical AERONET almucantur inversions, and found that global fine-mode dominated aerosol could be separated into three types, varying primarily by single scattering albedo (SSA or ω_0). There was a 'non-absorbing' aerosol model ($\omega_0\sim$0.95) that presumably corresponded to urban aerosol in the industrialized northern hemisphere, an 'absorbing' ($\omega_0\sim$0.85) aerosol model found in the known savanna-burning regions of South America and Africa, and a 'neutral' aerosol model found in primarily forest fire regions and the developing world. A similar analysis of spheroid retrievals showed that only a single model was necessary to describe the properties of presumably dust aerosol. They then 'fixed' the aerosol type

at a given season and location, based on the dominant aerosol type found during clustering. These decisions were mapped onto a 1° longitude x 1° latitude grid, such that a fine aerosol type is assumed for each grid point, globally. This global map approach, that is not hardwired into the processing code, allows for easy alterations as new information becomes available.

For the set of new assumed spherical fine aerosol models (absorbing, non-absorbing and neutral), Levy et al., (2006) computed the V5.2 LUT using a combination of MIEV (Wiscombe et al., 1980) and RT3 (Evans and Stephens, 1991). For the non-spherical (assumed spheroids) coarse (dust) aerosol they used the T-matrix code described in Dubovik et al., (2002, 2006). In addition, corrections for Rayleigh optical depths and center wavelengths were performed. The LUT was calculated for seven aerosol loadings ($\tau_{0.55}$ = 0.0, 0.25, 0.5, 1.0, 2.0 3.0, and 5.0), 9 solar zenith angles (θ_0 = 0.0, 6.0, 12.0, 24.0, 35.2, 48.0, 54.0, 60.0 and 66.0), 16 sensor zenith angles (θ = 0.0 to 66.0, increments of 6.0), and 16 relative azimuth angles (ϕ = 0.0 to 180.0 increments of 12.0). For specific AERONET sites, sun-derived spectral τ dependence were compared with the assumed models.

4. VIS/SWIR surface reflectance assumptions

When performing atmospheric retrievals from MODIS or any other satellite, the major challenge is separating the total observed reflectance into atmospheric and surface contributions (e.g. Equation 3), and then defining the aerosol contribution. Over the ocean, the surface is nearly black at red wavelengths and longer, so that assuming negligible surface reflectance in these channels is a good approximation. Over land, however, the surface reflectance in the visible and SWIR is far from zero and varies over surface type. As the land surface and the atmospheric signals are comparable, errors of 0.01 in assumed surface reflectance will lead to errors on the order of 0.1 in τ retrieval. Errors in multiple wavelengths can lead to poor retrievals of spectral τ, which in turn would be useless for estimating size parameters.

Kaufman and colleagues (e.g. Kaufman et al., 1997b) observed that over vegetated and dark soiled surfaces, the surface reflectance in some visible wavelengths correlated with the surface reflectance in the SWIR. Parallel simulations by vegetation canopy

models, showed that the physical reason for the correlation was the combination of absorption of visible light by chlorophyll and infrared radiation by liquid water in healthy vegetation (Kaufman et al., 2002). These relationships were such that the surface reflectance values in the visible were nearly fixed ratios of that in the SWIR (Kaufman et al., 1997b). As applied for C004, surface reflectance at $0.47\mu m$ (channel 3) and $0.66\ \mu m$ (channel 1) were assumed to be one-quarter and one-half, respectively, of the surface reflectance in the mid-SWIR $2.12\mu m$ (channel 7) (Kaufman et al., 1997b).

Regression of C004 (and prior) MODIS-derived τ to AERONET sunphotometer data (Chu et al., 2002; Remer et al., 2005) has shown that while the products generally agreed (~60-65%) to within the expected errors of Eq. 1 ($\pm 0.05 \pm 0.15\tau$), there was a positive offset of about 0.1 (Eq. 2). This means that the C004 algorithm generally over-estimates τ in pristine conditions, which questions the assumed surface reflectance. From data observed during the CLAMS experiment of 2001, Levy et al., (2005) found that higher values of VIS/SWIR surface ratios (e.g. 0.33 and 0.65 for the blue and red, respectively) improved the continuity of the MODIS over-land and over-ocean aerosol products along the coastline of the DelMarVa Peninsula. The MODIS/AERONET τ regression over near-coastal sites was also improved. However, at locations far from the coastline, the CLAMS VIS/SWIR ratios tended toward over-correction of the surface reflectance and retrievals of τ less than zero. Thus, we know that a single ratio is not globally applicable.

It is known that earth's surface is not Lambertian, and that some surface types exhibit strong bi-directional reflectance functions (BRDF). Gatebe et al., (2001) flew the Cloud Absorption Radiometer at low altitudes over vegetated surfaces and found that the VIS/SWIR surface ratios varied as a function of angle, and often greatly differed from the one-quarter and one-half ratios assumed in C004. Remer et al., (2001) also noted that the VIS/SWIR surface ratios varied as a function of scattering geometry. In fact, under certain geometry, the assumed VIS/SWIR surface relationship broke down completely.

To continue with this philosophy of using VIS/SWIR relationships to determine VIS surface reflectance, we will need to link VIS/SWIR relationships to geometry and to surface characteristics that we can measure from space without confusion from overlying aerosol layers. Note that alternative philosophies including using digital surface type models and global maps of measured spectral albedo were explored, but found to be less

useful in the aerosol retrieval than measured parameters and empirical relationships. However, in order to develop the empirical relationships we need a data base of *surface* reflectances that are representative of a wide range of global conditions. Before Terra launch such data were unavailable. Today, we can use the accumulation of MODIS data to derive a large database of surface reflectances.

4.1. Atmospheric correction of C-004 MODIS/AERONET co-located products

Atmospheric correction (Kaufman and Sendra, 1988) attempts to calculate the optical properties of the surface, by theoretically subtracting the effects of the atmosphere from the satellite-observed radiation field. One needs to assume the optical properties of the intervening atmosphere, including all aerosol and non-aerosol components. In addition to knowing or assuming all atmospheric components, accurate radiative transfer (RT) is also required. The atmospherically corrected surface reflectance ρ^s_λ is calculated by re-arranging Eq. 3.

In order to minimize errors arising from multiple scattering by the aerosol, we have limited our atmospheric corrections to conditions of τ in the green less than 0.2. Out of the original 15,000 co-located MODIS/AERONET points (described in section 2), there are over 10,000 collocations with low τ. The archive includes the 'gas absorption corrected' MODIS-Level 2 observed reflectance, as well as AERONET-observed (L2A) spectral τ and column water vapor depth. For atmospheric correction we use the same reflectances that the MODIS algorithm used to retrieve the τ in the 10 km box that contains the AERONET instrument. These reflectances have been corrected for gas absorption, and clouds, snow, inland water and bright surfaces have been eliminated. , Aerosol and water vapor characteristics for the correction are provided by AERONET observations in that 10 km box. The AERONET data is average over an hour, centered at over pass time. The molecular properties of the atmosphere are assumed those of the U.S. standard atmosphere, with the Rayleigh optical depth (ROD) values scaled from sea level values,-according to the elevation/air pressure of the sunphotometer.

The relation between the satellite-measured reflectance and the surface reflectance is a complicated function of the atmospheric effects of scattering and absorption by the aerosol. Previous atmospheric correction exercises often assumed some form of the Continental aerosol model (e.g. Vermote et al. 1997), to describe both the scattering and absorption properties. While this model may provide reasonable simulations in blue and red wavelengths, it cannot be expected to provide accurate simulations in the MODIS 2.12 μm channel, especially for either extreme of fine or coarse –dominated aerosol conditions. Instead, we used AERONET-derived Ångstrom exponent (α) to decide whether the scene was fine or coarse aerosol. The 'neutral' (generic/developing world; SSA ~ 0.9) aerosol type (Levy et al. 2006) was assumed for the 4200 cases where α>1.6. Values of α< 0.6 led to assuming the coarse (dust) model (about 400 cases). Co-locations where 0.6<α<1.6 (about 6000 cases) were not used due to uncertainties of aerosol mixing.

4.2. Mean values of VIS/SWIR surface reflectance relationships

Atmospheric correction was performed on the 4600 MODIS/AERONET co-locations having $\tau_{0.55}$<0.2 and α<0.6 or α>1.6. Figure 1 plots the entire set of atmospherically corrected visible surface reflectance (in the blue $\rho^s_{0.47}$ and the red $\rho^s_{0.66}$) versus that in the mid-SWIR ($\rho^s_{2.12}$) and their regression lines. While not plotted, also considered were the regressions if they were forced through zero, thereby assuming that zero SWIR reflectance is zero reflectance over the entire spectrum (which would be equivalent to deriving simple ratios). Correlation (R) values are 0.93 for the red, but only about 0.75 for the blue. In the blue, forcing a regression through zero is quite different than that not constrained. If forced through zero, the slope tends toward 0.36, whereas including the offset (about +0.011) yields a slope closer to the assumed one-quarter (0.258). In the red, whether including offset or not, the slope is about 0.55. Thus in a mean sense, atmospheric correction of MODIS data yields VIS/SWIR surface reflectance relationships that differ substantially from the assumed C004 VIS/SWIR ratios. Fitting blue to red (Figure 8b) has higher correlation and less scatter than blue to SWIR, specifically $R = 0.87$. There is less difference between fitting through zero and not, such

that a straight blue/red ratio is about 0.54, and the full regression has slope = 0.508 and offset = 0.008. Therefore, instead of the 0.47 μm and 0.66 μm surface reflectance being calculated separately from 2.12 μm, we will calculate the 0.66 μm surface reflectance from that in 2.12 μm, followed by calculating 0.47 μm from the 0.66 μm, i.e.

$$\rho^s_{0.66} = f(\rho^s_{2.12})$$
$$\rho^s_{0.47} = g(\rho^s_{0.66}) \quad , \tag{4}$$

where f() and g() are two independent relationships. To test the robustness of the relationship we performed similar regression with only the 2058 points where $\tau_{0.55} < 0.1$. The relationship stayed nearly the same, except with slightly higher correlation values.

4.3. Variability of VIS/SWIR surface reflectance relationships: Angle

As noted in Fig. 1 the VIS/SWIR surface reflectance regressions display large scatter. For example, where 2.12 μm surface reflectance is 0.15, simply assuming the mean values of the red/SWIR and blue/red relationships would result in estimating the 0.66 μm surface reflectance as 0.083 and 0.47 μm surface reflectance of 0.050. The scatter plots show that in reality, the 0.66 μm reflectance could vary between approximately 0.05 and 0.1, and the 0.47 μm surface reflectance between 0.01 and 0.07. Obviously, this could result in very large errors in retrieved τ, on the order of 0.1 or 0.2 or more. Therefore, to reduce the scatter we look for dependencies on other parameters to refine the relationships.

Gatebe et al. (2002) and Remer et al. (2001) suggest that the VIS/SWIR surface reflectance relationships are angle dependent. Out of different possible angle parameters (solar zenith angle, sensor zenith angle, glint angle or scattering angle) we found that the scattering angle had the largest influence on the VIS/SWIR surface reflectance relationship. The scattering angle, Θ, is defined as:

$$\Theta = \cos^{-1}(-\cos\theta_0 \cos\theta + \sin\theta_0 \sin\theta\cos\phi) \tag{5}$$

where θ_0, θ and ϕ are the solar zenith, sensor view zenith and relative azimuth angles, respectively. The data from Fig.1 were sorted according to scattering angle and put into 20 groups of equal size (about 230 points for each scattering angle bin). Fig. 2 (a) displays the median values of surface reflectance in each bin as a function of scattering angle, and shows a definite relationship at 2.12 μm, less at 0.66 μm, and nearly none at 0.47 μm. Since Fig.1 showed that both a slope and y-offset was necessary to regress VIS and SWIR surface reflectance, we look for scattering angle dependence on both parameters. Fig 2 (b-d) plots the slope, y-offset and correlation of the surface reflectance relationships calculated in each scattering angle bin and plotted as a function of scattering angle. The $\rho^s_{0.66}$ / $\rho^s_{2.12}$ regression slope (r0660 in the figure) shows dependence on scattering angle, whereas the $\rho^s_{0.47}$ /$\rho^s_{0.66}$ regression slope (rVIS in the figure) shows nearly none. The regressed y-intercept shows strong dependence on scattering angle for both relationships. Especially interesting is that the red/SWIR y-offset goes from positive to negative with increasing scattering angle, with a value of zero near $\Theta=135°$.

4.4. Variability of VIS/SWIR surface reflectance relationships: Surface type and MVI

Because AERONET sites are located in different surface type regimes, it could be expected that the VIS/SWIR surface relationships will vary based on surface type and/or season. Using the International Geosphere/Biosphere Programme's (IGBP) scene map of USGS surface types and formatted for MODIS validation (http://edcdaac.usgs.gov/modis/mod12c1v4.asp), we determined the scene type of the MODIS/AERONET validation box. We then separated urban from non-urban surfaces, and grouped into season (winter or summer) and general location (mid-latitude or tropical). Generally, "greener" surfaces (midlatitude summer sites both urban and nonurban) have higher red to SWIR ratios (red/SWIR>0.55) than winter sites (red/SWIR<0.55) or tropical savannas and grasslands. As for the blue to red channel surface reflectance relationships, except for the urban sites during summer (blue/red ratio ~ 0.766), the relationships around the globe are relatively consistent (blue/red ~ 0.52).

Except for urban areas, most surfaces seem to have VIS/SWIR surface reflectance relationships that vary as a function of their "greenness." Can we relate the surface reflectance relationships to a vegetation index (VI)? The Normalized Difference Vegetation Index (NDVI), defined as a function of the red (0.66 μm – channel 1) and near-IR (0.86 μm – channel 2), can be heavily influenced by aerosol (Reference). An alternative is the $NDVI_{SWIR}$, defined as:

$$NDVI_{SWIR} = (\rho_{1.24}^m - \rho_{2.12}^m)/(\rho_{1.24}^m + \rho_{2.12}^m) \qquad (6)$$

where $\rho_{1.24}$ and $\rho_{2.12}$ are the MODIS-measured reflectances of the 1.24 μm channel (MODIS channel 5) and the 2.12 μm channel (channel 7), which are much less influenced by aerosol (except for heavy aerosol or dusts). This index is also known as $NDVI_{MIR}$ (Mid-InfraRed) in the work of Miura et al. (1998) and others. In aerosol free conditions $NDVI_{SWIR}$ is highly correlated with regular $NDVI$. A value of $NDVI_{SWIR} > 0.6$ is a highly vegetated area, whereas $NDVI_{SWIR} < 0.2$ is representative of sparse vegetation. Figure 3 plots the relationship of the 0.66 μm channel and 2.12 μm channel (atmospherically corrected) surface reflectance relationship, for nonurban sites, as a function of low, medium and high values of $NDVI_{SWIR}$. Clearly, as the $NDVI_{SWIR}$ increases, the ratio between 0.66 μm and 2.12 μm surface reflectance increases, and we will use this relationship in the final VIS/SWIR surface reflectance parameterization.\

4.5. Final parameterization of VIS/SWIR surface reflectance relationships

Results of the global atmospheric correction exercise imply that not only do the VIS/SWIR surface relationships differ from the ratios assumed by C004, they also have a strong dependence on both geometry and surface type. The new (V5.2) VIS/SWIR surface reflectance relationship is parameterized as a function of both $NDVI_{SWIR}$ and scattering angle Θ, such that Equation 4 can be expanded:

$$\rho_{0.66}^s = f(\rho_{2.12}^s) = \rho_{2.12}^s * slope_{0.66/2.12} + yint_{0.66/2.12}$$
$$\text{and}$$
$$\rho_{0.47}^s = g(\rho_{0.66}^s) = \rho_{0.66}^s * slope_{0.47/0.66} + yint_{0.47/0.66}$$

$$(7)$$

where

$$slope_{0.66/2.12} = slope_{0.66/2.12}^{NDVI_{SWIR}} + 0.002\Theta - 0.27,$$
$$yint_{0.66/2.12} = 0.00025\Theta + 0.033,$$
$$slope_{0.47/0.66} = 0.49, \text{and}$$
$$yint_{0.47/0.66} = 0.005$$

$$(8)$$

where in turn

$$slope_{0.66/2.12}^{NDVI_{SWIR}} = 0.48; NDVI_{SWIR} < 0.25,$$
$$slope_{0.66/2.12}^{NDVI_{SWIR}} = 0.58; NDVI_{SWIR} > 0.75$$
$$slope_{0.66/2.12}^{NDVI_{SWIR}} = 0.48 + 0.2(NDVI_{SWIR} - 0.25); 0.25 \le NDVI_{SWIR} \le 0.75$$

$$(9)$$

Note that while the above parameterization was based on the results of Figs 1-3, the coefficients are not identical to those in the figures. The atmospheric corrected data set is the broadest and most comprehensive representation of global surface reflectance relationships, still it is limited to AERONET site locations, which are in turn are mostly concentrated in certain geographical regions. Trial and error was used to modify the basic results from the AERONET-based atmospheric correction, to give more realistic MODIS retrievals globally, (especially in places were few or no AERONET sites are located).

4.6. Notes on VIS/SWIR surface reflectance relationship errors

We note that even with the surface reflectance parameterization, there still will be errors in estimating surface reflectance. According to the MODIS Land Surface Reflectance Homepage (http://modis-sr.ltdri.org/html/prodacc.htm), improper aerosol model assumptions can lead to errors in atmospherically corrected reflectance on the order of 0.002 in the 0.47 and 0.66 μm channels, and 0.006 at 2.12 μm. The errors are especially large at 2.12 μm due to potentially choosing a fine-dominated model instead of a coarse-dominated model (or vice-versa). However, since our study pre-determined the

choice of fine or coarse-dominated aerosol models via the AERONET-observed Ångstrom exponent, presumably errors at 2.12 μm should be much less. The difference in spectral optical thickness between the V5.2 fine-dominated neutral and absorbing models (at $\tau_{0.55}$=0.5) is about 0.02, 0.02 and 0.002, respectively in the 0.47, 0.66 and 2.12 μm channels. On average, this would be equivalent to errors of 0.002, 0.002 and 0.0002, respectively in surface reflectance, but would vary according to the differences in phase function. Regardless, the error at 2.12 μm is small enough so that the derived surface reflectance relationship should be reasonably robust.

Of course, other errors may creep into the surface reflectance parameterization. These include, but are not limited to additional surface BRDF effects lost during averaging over scattering angle and errors due to MODIS instrument calibration. The MODIS Land Surface Reflectance Homepage suggests that these errors can cause reflectance errors that similar in magnitude to those caused by improper aerosol model assumptions.

5. Inversion of spectral reflectance: The V5.2 algorithm

A major limitation of the old C004 algorithms is that aerosol is assumed transparent in the 2.12 μm SWIR channel. The surface reflectance in 2.12 μm is assumed to be exactly the value of the observed TOA reflectance in that channel. Under a dust aerosol regime, aerosol transparency is an extremely poor assumption. Even in a fine aerosol dominated regime, τ is not zero. For example, for our "generic/developing world" (neutral ω_0~0.90) aerosol, $\tau_{0.55}$ of 1.0 corresponds to $\tau_{2.12}$ of 0.114. For a given angle (say $\theta_0 = 36°$, $\theta = 36°$, and $\phi = 72°$) assuming $\tau_{2.12} = 0.0$ instead leads to error in 2.12 μm path reflectance of about 0.012. Via the VIS/SWIR reflectance relationship, the reflectance error at 0.66 μm would be on the order of 0.006, leading to ~ 0.06 error in retrieved τ. As a percentage of the actual τ, the error is not very large. However, combined with errors at 0.47 μm, the resulting incorrect Ångstrom exponent leads to error in estimating η.

In the spirit of the MODIS aerosol over ocean algorithm (Tanré et al., 1997), we developed a multi-channel reflectance inversion for retrieving aerosol properties over land. Analogous to the ocean algorithm's combination of fine and coarse aerosol *modes*, the V5.2-land algorithm attempts to combine fine-dominated and coarse-dominated

aerosol *models* (each composed of multiple modes) to match with the observed spectral reflectance. The 2.12 μm channel is assumed to contain both surface and aerosol information, and the visible surface reflectance is a function of the new V5.2 VIS/SWIR surface reflectance relationships. Simultaneously inverting the aerosol and surface information in the three channels (0.47 μm, 0.66 μm and 2.12 μm) yields three parameters: $\tau_{0.55}$, $\eta_{0.55}$ and the surface reflectance ($\rho^s_{2.12}$).

We rewrite equation 3, but note that the calculated spectral total reflectance ρ^*_λ at the top of the atmosphere is the weighted sum of the spectral reflectance from a combination of fine and coarse –dominated aerosol models, i.e.

$$\rho^*_\lambda = \eta \rho^{*f}_\lambda + (1-\eta)\rho^{*c}_\lambda \qquad (10)$$

where ρ^{*f}_λ and ρ^{*c}_λ are each composites of surface reflectance ρ^s_λ and atmospheric path reflectance of the separate aerosol models. That is:

$$\rho^{*f}_\lambda = \rho^{af}_\lambda + F^f_{d\lambda} T^f_\lambda \rho^s_\lambda / (1 - s^f_\lambda \rho^s_\lambda)$$
$$\text{and} \qquad (11)$$
$$\rho^{*c}_\lambda = \rho^{ac}_\lambda + F^c_{d\lambda} T^c_\lambda \rho^s_\lambda / (1 - s^c_\lambda \rho^s_\lambda)$$

where ρ^{af}_λ and ρ^{ac}_λ are the fine and coarse model atmospheric path reflectance, $F^f_{d\lambda}$ and $F^c_{d\lambda}$ are normalized downward fluxes for zero surface reflectance, T^f_λ and T^c_λ represent upward total transmission into the satellite field of view, and s^f_λ and s^c_λ are atmospheric backscattering ratios. The weighting parameter, η in Eq. 10, is defined for λ = 0.55 μm. In the appendix of Remer et al. (2005) they show how this parameter also represents the fraction of the total optical thickness at 0.55 μm contributed by fine model aerosol. Note the angular and τ dependence of some of the terms: $\rho^a = \rho^a(\tau, \theta_0, \theta, \phi)$, $F = F(\tau, \theta_0)$, $T = T(\tau, \theta)$, $s = s(\tau)$ and $\rho^s = \rho^s(\theta_0, \theta, \phi)$. Whereas the other terms are a function of the aerosol properties (not aerosol amount) and are contained within the lookup tables. The surface reflectance is independent of the aerosol, but dependent on the geometry. In practical terms, we parameterize the surface reflectance through the VIS/SWIR surface reflectance relationships, which causes it to be a function of scattering angle and vegetation index.

Due to the limited set of aerosol optical properties in the lookup table, the equations may not have exact solutions, and solutions may not be unique. Therefore, we

17

find the aerosol solution most closely resembling the set of MODIS measured reflectance. In order to reduce the possibility of non-unique retrievals we only allow discrete values of η. Upon completion, the retrieval is assigned a Quality Assurance 'confidence' (QAC) value that ranges from 0 (bad quality) to 3 (good quality). This QAC flag is used for creation of Level 3 (gridded) products and for combining land retrievals with concurrent over-ocean aerosol retrievals into 'joint products'

5.1. Selection of "dark pixels"

Figure 4 illustrates the main steps of the V5.2 land algorithm. Each individual MODIS scene, called a granule, consists of a 5-minute swath of data, measuring approximately 1340 km by 2030 km. The relevant Level 1 B (L1B) data include calibrated spectral reflectance in eight wavelength bands at a variety of spatial resolutions, as well as the associated geo-location information. The spectral data include the 0.66 and 0.86 μm channels (MODIS channels 1 and 2 at 250 m resolution), the 0.47, 0.55, 1.24, 1.64 and 2.12 μm channels (channels 3, 4, 5, 6 and 7 at 500 m), and the 1.38 μm channel (channel 26 at 1 km). The geo-location data are at 1 km and include angles $(\theta_o, \theta, \phi,$ and $\Theta)$, latitude, longitude, elevation and date. Θ is the scattering angle. The L1B reflectance values are corrected for water vapor, ozone, and carbon dioxide (described in Remer et al. 2006) before proceeding.

The first step is to organize the measured reflectance into nominal 10 km by 10 km boxes (corresponding to 20 by 20, or 40 by 40 pixels, depending on the channel). The 400 pixels in the box are evaluated pixel by pixel to identify whether the pixel is suitable for aerosol retrieval. Clouds (Martins et al., 2002), snow/ice (Li et al., 2004) and inland water bodies (via NDVI tests) are considered not suitable and are discarded. Details of this masking are also described in Remer et al. (2006).

The non-masked pixels are checked for their brightness. Pixels having 2.12 μm measured reflectance between 0.01 and 0.25 are grouped and sorted by their visible reflectance. The brightest (in the visible) 50% and darkest 20% are discarded, in order to reduce cloud and surface contamination and scale towards darker targets. If there are at least 12 pixels remaining (10% of 30% of the original 400), then the reflectance in each

channel is averaged, yielding the "MODIS-measured" spectral reflectance $\rho^m{}_{0.47}$, $\rho^m{}_{0.66}$, $\rho^m{}_{2.12}$, and $\rho^m{}_{1.24}$. These reflectance values are used for Procedure A. If less then 12 pixels remain, then Procedure B (described later) is followed.

5.2. Correcting the LUT for elevation

A major change from the old C004 concerns how the algorithm corrects for elevated surface targets. The sea-level Rayleigh optical depth (ROD, $\tau_{R,\lambda}$) at a wavelength λ (in μm) can be approximated over the visible range (e.g. Dutton et al., 1994; Bodhaine et al., 1999) by:

$$\tau_{R,\lambda} = 0.00877\lambda^{-4.05} \tag{12}$$

When not at sea level (pressure = 1013 mb), the ROD is a function of pressure (or height, z) so that it can be approximated by:

$$\tau_{R,\lambda}(z = Z) = \tau_{R,\lambda}(z = 0)\exp(\frac{-Z}{8.5}) \tag{13}$$

where Z is the height (in kilometers) of the surface target and 8.5 km is the exponential scale height of the atmosphere. The difference between ROD at z=0 and z=Z is $\Delta\tau_{R,\lambda}$.

In C004, the algorithm (too) simply corrected the retrieved τ product by adding the optical depth that was neglected by assuming sea level for the retrieval, (i.e. $\tau_\lambda(z = Z) = \tau_\lambda(z = 0) + \Delta\tau_{R,\lambda}$). However, this correction can give poor results because of the large differences between molecular and aerosol phase functions. Instead, the V5.2 algorithm makes use of the procedure described in Fraser et al., (1989). The algorithm adjusts the lookup table to simulate different ROD by adjusting the wavelength. Substitution of equation 12 into equation 13 yields

$$\lambda(z = Z) = \lambda(z = 0)\exp(\frac{Z}{34}). \tag{14}$$

For example, at Z = 0.4 km, λ increases by about 1.2%. For the blue 0.47 μm channel, (centered at 0.466 μm) this means that $\tau_{R,\lambda}(z = 0) = 0.194$, $\tau_{R,\lambda}(z = 0.4) = 0.185$

and $\lambda(z = 0.4) = 0.471$ µm. In other words, the algorithm simulates an elevated surface by adjusting the blue channel's wavelength to 0.471 µm. Assuming that gases and aerosols are optically well mixed in altitude, the algorithm substitutes for the parameter values of the 0.47 µm LUT by interpolating (linearly as functions of log wavelength and log parameter) between the 0.47 µm (0.466 µm) and the 0.55 µm (0.553 µm) entries. Similar interpolations are performed for the other channels (for example, 0.55 µm would be adjusted to 0.559 µm). For the 0.4 km case, this means that lower values of TOA atmospheric path reflectance and higher values of transmission are chosen to represent a given aerosol model's optical contribution. However, also note that since the 0.55 µm channel has also been adjusted, the associated values of the τ indices have been adjusted accordingly.

Whereas most global land surfaces are at sea level or above, a few locations are below sea level ($Z < 0$). In these cases, the algorithm is allowed to extrapolate below 0.466 µm. Since the extrapolation is at most for a hundred meters or so, this is not expected to introduce large errors, and these cases can still be retrieved. Note also that due to the extremely low ROD in the 2.12 µm channel, little is gained by adjusting this channel.

5.3. Procedure A: Inversion for dark surfaces

If following Procedure A (for dark surfaces), the QAC is initially set to a value between 0 (bad quality) and 3 (good quality), depending on the number of dark pixels remaining. In Procedure A, the algorithm assigns the fine aerosol model, based on the location and time (Levy et al. 2006). From the lookup table, ρ^a, F, T and s (for the fine model and coarse model separately) are interpolated for angle, resulting in six values for each parameter, each one corresponding to a different aerosol loading (indexed by τ at 0.55 µm).

The 2.12 µm path reflectance is a non-negligible function of the τ, so that the surface reflectance is therefore also a function of the τ.   For discrete values of η between -0.1 and 1.1 (intervals of 0.1), the algorithm attempts to find the τ at 0.55 µm and the surface reflectance at 2.12 µm that exactly matches the MODIS measured

reflectance at 0.47 μm. There will be some error, ε, at 0.66 μm. The solution is the one where the error at 0.66 μm is minimized. In other words,

$$\rho_{0.47}^m - \rho_{0.47}^* = 0$$

$$\rho_{0.66}^m - \rho_{0.66}^* = \varepsilon \qquad\qquad \text{(15abc)}$$

$$\rho_{2.12}^m - \rho_{2.12}^* = 0$$

where

$$\rho_{2.12}^* = \eta(\rho_{2.12}^{fa} + F_{d2.12}^f T_{2.12}^f \rho_{2.12}^f /(1 - s_{2.12}^f \rho_{2.12}^s)) + (1 - \eta)(\rho_{2.12}^{ca} + F_{d2.12}^c T_{2.12}^c \rho_{2.12}^s /(1 - s_{2.12}^c \rho_{2.12}^s))$$

$$\rho_{0.66}^* = \eta(\rho_{0.66}^{fa} + F_{d0.66}^f T_{0.66}^f f(\rho_{2.12}^s) /(1 - s_{0.66}^f f(\rho_{2.12}^s))) + (1 - \eta)(\rho_{0.66}^{ca} + F_{d0.66}^c T_{0.66}^c f(\rho_{2.12}^s) /(1 - s_{0.66}^c f(\rho_{2.12}^s)))$$

and

$$\rho_{0.47}^* = \eta(\rho_{0.47}^{fa} + F_{d0.47}^f T_{0.47}^f g(\rho_{0.66}^s) /(1 - s_{0.47}^f g(\rho_{0.66}^s))) + (1 - \eta)(\rho_{0.47}^{ca} + F_{d0.47}^c T_{0.47}^c g(\rho_{0.66}^s) /(1 - s_{0.47}^c g(\rho_{0.66}^s))),$$

$$\text{(16abc)}$$

where in turn, $\rho^a = \rho^a(\tau)$, $F = F(\tau)$, $T = T(\tau)$, $s = s(\tau)$ are functions of τ indices in the lookup table that is calculated separately for fine and coarse models. $f(\rho_{2.12}^s)$, $g(\rho_{0.66}^s)$ are described by Equations 7-9. Note that non-physical values of η are tried (-0.1 and 1.1) to allow for the possibility of inappropriate assumptions in either aerosol models or surface reflectance. Again, the primary products are $\tau_{0.55}$, $\eta_{0.55}$, and the surface reflectance ($\rho_{2.12}^s$). The error ε is also noted.

5.4. Procedure B: Alternative Retrieval for Brighter surfaces

The derivation of aerosol properties is possible when the 2.12 μm reflectance is brighter than 0.25, but is expected to be less accurate (Remer et al., 2005), due to increasing errors in the VIS/SWIR relationship. However, if Procedure A was not possible, but there are at least 12 cloud-screened, non-water pixels, satisfying

$$0.25 < \rho_{2.12}^m < 0.25G < 0.40 \qquad\qquad \text{(17)}$$

where

$$G = 0.5((1/\mu) + (1/\sqrt{\mu_0})) \ , \qquad\qquad (18)$$

then Procedure B is attempted. In this relationship μo is cosine of the solar zenith angle, $\cos(\theta_o)$, and μ is cosine of the satellite view angle, $\cos(\theta)$. In procedure B, the QAC is automatically set to 0 ("bad quality").

Procedure B is analogous to "Path B" described in Remer et al., (2005). Like in C004, the Continental aerosol model is assumed. Unlike C004, the VIS/SWIR surface reflectance assumptions are those described by Equations 7-9, and the Continental aerosol properties are indexed to 0.55 μm. In other words, V5.2 uses equations 10-11, except with the first term only (i.e. $\eta = 1.0$). The primary products for Procedure B are τ $(\tau_{0.55})$ and the surface reflectance $(\rho^s_{2.12})$. The error ε is also saved.

5.5. Derivation of Fine Mode τ, Mass Concentration and other secondary parameters

Following the derivation of primary products by Procedure A $(\tau_{0.55}, \eta_{0.55}$ and $\rho^s_{2.12})$, a number of secondary products can also be calculated. These include the fine and coarse mode optical depths $\tau^f_{0.55}$ and $\tau^c_{0.55}$:

$$\tau^f_{0.55} = \tau_{0.55}\eta_{0.55} \quad \text{and} \quad \tau^c_{0.55} = \tau_{0.55}(1 - \eta_{0.55}) \qquad\qquad (19)$$

the mass concentration, M:

$$M = M^f_c \tau^f_{0.55} + M^c_c \tau^c_{0.55} \qquad\qquad (20)$$

the spectral total and model optical thicknesses τ_λ, τ^f_λ and τ^c_λ:

$$\tau_\lambda = \tau^f_\lambda + \tau^c_\lambda$$
$$\text{where} \qquad\qquad (21)$$
$$\tau^f_\lambda = \tau^f_{0.55}(Q^f_\lambda / Q^f_{0.55}) \quad \text{and} \quad \tau^c_\lambda = \tau^c_{0.55}(Q^c_\lambda / Q^c_{0.55})$$

the Ångstrom Exponent α:

$$\alpha = \ln(\tau_{0.47}/\tau_{0.66})/\ln(0.466/0.644) \qquad\qquad (22)$$

and the spectral surface reflectance ρ^s_λ, computed by re-arranging Equations 7-9. M^f_c and M^c_c are mass concentration coefficients for the fine and coarse mode, whereas Q^f_λ and Q^c_λ represent model extinction coefficients at wavelength, λ. If the resulting products are inconsistent, then the QAC value initially assigned to the pixel is changed to 0 ('bad quality'). If Procedure B was followed, the only secondary products calculated are M and $\tau_{0.47}$, and the QAC is set to 0. The other products in Procedure B are left undefined. Levy et al., (2006) describe how the Q and M_c coefficients are defined.

5.6. Low and negative optical depth retrievals

A major philosophical change from C004 to C005 is that negative τ retrievals are allowed. Given that there is both positive and negative noise in the MODIS observations, and that surface reflectance and aerosol properties may be under or over-estimated depending on the retrieval conditions, it is statistically useful to allow retrieval of negative τ. In fact it is necessary for creating an unbiased dataset from any instrument. Without negative retrievals the τ dataset is biased by definition. However, a large negative retrieval indicates a situation outside the algorithm's solution space and should not be reported.The trick is to determine the cutoff between a retrieved τ that is essentially the same as zero, and a retrieved τ that is truly wrong. MODIS should retrieve with the expected error defined by Equation 1, then values down to -0.05 are essentially the same as a zero retrieval and are reported as retrieved. Allowing for slightly higher uncertainty, we include τ retrievals down to -0.10 (twice the expected error in pristine aerosol conditions), but report these values as -0.05 and lower the QAC value. Note that all retrievals with $-0.05 < \tau < 0$ are reported with high QAC value $= 3$, unless identified as poor quality for some other reason. Some of the products that are retrieved or derived (such as η or Ångstrom Exponent) are set to zero or reported as not defined for negative retrievals. In cases of low τ ($\tau < 0.2$), η is too unstable to be retrieved with any accuracy. Therefore, η is reported as un-defined even though other parameters (such as Ångstrom exponent and Fine τ) may be reported.

5.7. Sensitivity study

Following the lead of Tanré et al (1997), we have tested the sensitivity of Procedure A by applying it for the following exercises: (1) simulation of conditions that are included within the LUT, (2) simulations where one of the parameters (i.e. τ) is not included within the LUT, and (3) simulations for conditions that include one or more errors.

Exercise 1: Whereas the study of Tanré et al, (1997) tested the algorithm on a single geometrical combination, we performed the study in (1) by simulating the 720 reasonable geometrical combinations in the LUT ($0° \leq \phi \leq 180°$, $\theta \leq 60°$, $\theta_0 \leq 48°$). We assumed the "fine" aerosol model to be the neutral (SSA ~ 0.9) aerosol model and that the "coarse" model was our Spheroid (dust) model (Levy et al. 2006). For each combination of geometry, and for each MODIS channel, we extracted the fine and coarse mode values of atmospheric path reflectance ρ^a_λ, backscattering ratio s_λ, downward flux F_d and transmission T_λ. We assumed that the 2.1 μm surface reflectance $\rho^s_{2.12} = 0.15$, and the C004 VIS/SWIR surface reflectance ratios (i.e, $\rho^s_{0.66} = 0.5 \, \rho^s_{2.12}$ and $\rho^s_{0.47} = 0.5 \rho^s_{0.66}$). Using Equations 10-11, we simulated TOA reflectance ρ^*_λ for 5 discrete values of η ($\eta = 0.0, 0.25, 0.5, 0.75$ and 1.0). Therefore, for each value of τ in the LUT, there are 720 x 5 = 3600 attempts to retrieve that τ.

For smaller τ ($\tau \leq 1$), the τ was retrieved within $\Delta\tau < 0.01$ for all 3600 attempts. As τ increases, however, computational instabilities lead to a less exact solution. Still, though, the retrieved τ is certainly within 10% and in most cases to within $\Delta\tau < 0.1$. When we hold τ constant ($\tau = 0.5$) and attempt to retrieve values of η within the LUT ($\eta = 0.0$ or 1.0) for the 720 geometrical combinations, we find that η is retrieved exactly.

Figs 5 and 6 provide another way of assessing the retrieved MODIS products. Fig. 5 plots retrieved τ, surface reflectance and fitting error as a function of either air mass (top) or scattering angle (bottom), given that the input conditions are $\tau_{0.55} = 0.5$, $\eta = 0.5$ and $\rho^s_{2.12} = 0.15$. In this case, we plotted all of the 720 geometrical combinations in the LUT. Air mass is defined as $1/\cos(\theta_0)$. The retrieval never exactly matches the input reflectances, although the errors are very small (less than 0. 1%). Note that the retrieval uses an under-estimated surface reflectance to balance the over-estimated optical depth.

Fortunately, though, most errors are small, and are well within any expected error bars. Fig 6 is similar, but for $\eta=0.25$, and plotted only for the air mass dependence. The errors are much larger (up to 1%), but τ is still well within expected error.

Exercise 2. We used the same combination of radiative transfer codes (MIEV + RT3) used for the LUT (Levy et al., 2006) to simulate additional values of aerosol loading ($\tau_{0.55} = 0.35$, 1.5 and 6.0) to create an "extended" LUT. As in exercise (1) we simulated the same 720 geometrical combinations as in the V5.2 LUT and the five values of η. On average the retrieval is very close to the expected value, however, the standard deviation over all geometry is larger than for τ in the normal LUT. A notable exception is the attempt at retrieving $\tau_{0.55} = 6.0$, where the algorithm does a poor job of extrapolating. In the operational algorithm, we constrain the maximum possible τ to be 5.0. As for retrieving values of η not included in the V5.2 LUT, the algorithm is successful. The $\eta=0.5$ retrieval is well behaved. The attempt at resolving either $\eta=0.25$ or $\eta=0.75$ leads to retrieving $\eta=0.20$ and $\eta=0.70$. Although it is impossible for an exact retrieval, due to the algorithm choosing between 0.1 intervals, it is interesting that no retrievals of $\eta=0.30$ or $\eta= 0.80$ are produced.

Exercise 3. This exercise studied the impact of different types of errors that could creep into the retrieval process. Potential errors include (but are not limited to) random, systematic or spectrally dependent errors that arise from issues like sensor calibration, assuming the wrong aerosol model at a given location, coarse input topography mapping, or wrong estimates of the VIS/SWIR surface reflectance relationships. These errors are expressed by adding random or systematic errors in the measurements of one or more spectral channels, geometrical conditions or other input boundary conditions. Table 1 lists some prescribed errors, and Table 2 lists eight sample geometries used in this exercise. Table 3 shows results when attempting to retrieve conditions of $\tau_{0.55}=0.5$, $\eta=0.5$ and $\rho^{s}_{2.12}=0.15$, for the eight sample geometries described in Table 2. Table 3A displays the retrieved values of $\tau_{0.55}$ for each case. Table 3B shows the Mean Squared Error (MSE) for each retrieved product, computed over all eight geometries. For any case of prescribed errors/geometry, one or more products may be over-estimated or under-estimated. If all geometry leads to either one direction or the other, the MSE value is designated by (+) or (-). For example, when retrieving with no

additional errors ('LUTinput'), τ is never retrieved exactly, but is over-estimated by an average MSE of 0.0011 (+). In balance, $\rho^s_{2.12}$ is consistently underestimated (MSE of 0.0004 (-)), with a nonzero fitting error, ε. This is simply a result of computer round off error.

Under most conditions, introducing minor calibration or random errors does not destroy the retrieval of τ. For most individual errors, the retrieved τ is accurate to within 0.02. However, even when we combine errors (model error, random error, surface error, calibration error and geometrical error), we still retrieve τ=0.5 with MSE = 0.10, thus retrieving within the expected error of $\Delta\tau$=0.125. Retrieval of surface reflectance seems to be extremely robust. Retrieval of η is much more unstable. For simple calibration and geometrical errors, the MSE for η is < 0.1. Combinations of errors lead to large MSE (>0.2) for η retrieval, meaning that η is not a stable product. Yet, these sensitivity tests indicate that generally, the V5.2 aerosol over land algorithm can retrieve useful products.

6. The aerosol products

Examples of the three primary aerosol products ($\tau_{0.55}$, η and $\rho^s_{2.12}$) are shown in Fig. 7, along with a color composite of the L1B reflectances (0.47, 0.55 and 0.66 μm channels). This image was taken on May 4, 2001 over the U.S. East Coast, and is the same image used by King et al., (2003). We note the continuity of the τ from land to ocean, and that the retrieval of η and surface reflectance seem reasonable. Note that η is not plotted over land when $\tau < 0.2$.

Table 4 lists the aerosol over land products that are contained in each "M?D04" L2 granule file (MOD04 for Terra and MYD04 for Aqua). For each product, the table lists its name within the file, its dimension, and its type. All products are at least two-dimensional (nominally 135 x 204 at 10 km x 10 km resolution), and many have three dimensions. If there is a third dimension, the channels (usually wavelengths) are listed. A parameter's type may be Retrieved, Derived, Diagnostic, Experimental, or Joint Land and Ocean. A *Retrieved* parameter is one that results directly from the inversion (Procedure A), whereas those *Derived* (such as the Ångstrom Exponent), result from those directly

retrieved. Products that are *Diagnostic* include QA parameters and those parameters that were calculated during intermediate steps. These diagnostic parameters can be used to understand how the retrieval worked. Products denoted *Experimental* are superfluous to the main inversion, may be useful for other applications, but are not discussed here. Finally, *Joint Land and Ocean* products are those that are composites of over-land and over-ocean aerosol retrievals. These are intended either for quantitative use (Quality Assured where QAC>0; e.g. Optical_Depth_Land_And_Ocean), or for qualitative imaging (QAC ≥ 0; e.g. Image_Optical_Depth_Land_And_Ocean).

7. Provisional validation of V5.2 products

The primary means of MODIS validation is by comparing the products with equivalent measurements from AERONET or other aerosol measurements. In this way, some of the products of C004 (i.e. V4.2 and before) were *validated* (e.g. Remer et al., 2005), meaning that they were demonstrated to be accurate to within certain errors. In the case of the land products (through V4.2), this meant that ~60% (slightly less than one standard deviation) of the AERONET-measured τ values were retrieved by MODIS to the expected error described by Equation 1. The other land parameters were either not yet validated, or are diagnostic parameters that cannot be validated.

Since that paper, the algorithm has gone through some minor updates. The last update to the C004 family was known as Version 5.1 ('V5.1'). V5.1 updated the snow mask (Li et al., 2005) and cleaned up confusing information in the output files. Even though V5.1 never became operational, it is being used in this paper to bridge between the operational C004 family of algorithms and the new algorithm we introduce in this paper. In addition to validation by AERONET, we make qualitative analyses based on visual inspection and global statistics.

7.1. Direct comparison of V5.2 and V5.1 products

Fig. 8 plots retrieved τ at 0.55 μm from both V5.1 and V5.2, over small areas of a MODIS granule. V5.1 (OLD) is presented in (a), whereas V5.2 (NEW) is shown in (b).

Fig. 8 shows a region in the western U.S. from 30 Sep 2003. The V5.2 aerosol retrieval adds more valid retrievals over very low τ areas (coastal Oregon and northern California). V5.2 reports these areas as having near zero or slightly negative τ, where V5.1 would have reported fill values (errors). In areas farther from the coastline, V5.2 tends to clean up contamination presumably caused by clouds, elevation, and inhomogeneous surface properties, and produces a much more reasonable picture of τ.

7.2. Statistics of V5.2 versus V5.1

Of most interest to the climate community will be the changes in the statistics of the aerosol products. These include the global mean values and the distribution (histogram) of the values. For the set of MODIS granules listed in Table 5 (about 6300 granules of both Terra and Aqua), the mean 0.55 μm τ is reduced from 0.28 to 0.21. This is a significant reduction that can be compared with model estimates.

Fig 9 plots the histograms of retrieved τ at 0.55 μm from both V5.1 and V5.2. These histograms include 141 individual Terra and Aqua granules that are known as the MODIS "test_bed", and twelve days of global data – all listed in Table 5. The use of global data is especially important for determining how the retrieval behaves in regions not selected for algorithm development. Of course, the obvious change in the V5.2 product is that small magnitude negative τ retrievals are valid. About 10-11% of the total τ retrievals are now retrieved as below zero, of which only about 3% are below -0.05. This promising result indicates that V5.2 has reasonable ability to detect very clean conditions within the expected error of ±0.05. Also noted in Fig 9 is that the fraction of retrieved medium to medium high τ (0.2 < τ < 0.75) is reduced, while the fraction of high τ (τ > 0.75) remains about the same.

7.3. Comparison of V5.2 to V5.1 and with AERONET

As of 1 April 2006, the V5.2 algorithm has been run on nearly 6300 granules, including one full month (August 2001), fifteen entire days (listed in Table 5) and about 141 individual granules that are known as the MODIS "test_bed." These granules include observations from both Terra and Aqua, and are seasonally and yearly representative of the MODIS time series. For comparison, we ran V5.1 on the same set of granules. Figures 10 and 11 plot the comparisons of both V5.1 and V5.2 with the AERONET data, via the spatio-temporal co-location method of Ichoku et al., (2002).

Figure 10 plots the retrieved MODIS τ against AERONET τ, both at 0.55 μm. The data have been sorted by AERONET τ and averaged into bins with equal numbers of observations in each bin. The mean and standard deviation of each bin are calculated and plotted in Fig. 12 as a solid dot and error bars. The correlation is calculated from the freely plotted points before binning, although the cloud of points is not shown in the plot. The regression equation has improved tremendously, from "y=0.097+0.91x" to "y=0.029+1.01x." Correlation R is also improved, from R=0.847 to R=0.894. It should be noted that slight differences in the number of points arise due to different selection of valid dark pixels and allowance of below zero τ retrievals.

Figure 11a plots MODIS η against AERONET η, where AERONET η is calculated from sun observations of spectral τ as described by O'Neill et al., (2003). Keep in mind that unlike MODIS/AERONET comparisons of τ, MODIS and AERONET do not retrieve the same quantity labeled as η. The AERONET retrieval assumes one fine mode and one coarse mode. Thus, AERONET η is the weighting between *modes*. The MODIS land η is a weighting between *models*, where fine-dominated models contained coarse modes and coarse-dominated models contain fine modes. The improvement to the MODIS η product is mainly its correlation to AERONET. Note that η is defined only when $\tau > 0.2$. Figs 11b and c show comparisons for derived products, including the Ångstrom Exponent (defined by 0.47 and 0.66 μm), and Fine optical depth (i.e. $\tau^f = \tau \times \eta$), respectively. For Fine τ, the correlation and slopes are nearly unchanged between V5.1 and V5.2; however, the offset goes from +0.051 to -0.031. The result is that nearly two-thirds of all V5.2 MODIS Fine τ fall within expected errors defined by Eq. 1. Note again that the difference in the number of points is due to different selection of dark pixels and treatment of negative τ retrievals. The Ångstrom exponent has little

improvement from V5.1 to V5.2, except for slightly better but still poor correlation with the AERONET measured quantities. In general, the changes to the MODIS aerosol retrieval algorithm described here have resulted in a much less biased τ and τ^f products than the previous algorithm. MODIS η correlates better with AERONET, although it still leaves room for improvement.

8. Conclusion

In this document, we have introduced a new algorithm (V5.2) for deriving aerosol optical properties over dark land surfaces, from MODIS observed spectral reflectance. In the new algorithm, we have updated a number of assumptions, including the VIS/SWIR surface reflectance parameterization, and the statistical implications of deriving below zero aerosol optical thickness. Most significantly, instead of an independent two-channel retrieval, V5.2 is a simultaneous three-channel inversion that makes use of aerosol information contained in the SWIR (2.12 μm) channel. We have coupled these changes with updated representative global aerosol optical models that are described in Levy et al. (2006).

The V5.2 algorithm has been tested, both for its theoretical ability to derive aerosol properties, and on a test bed of 6300 MODIS granules. Compared with co-located AERONET sites, the V5.2 MODIS algorithm retrieves aerosol properties more accurately than V5.1. Specifically, the retrievals of total τ meet expected accuracy levels ($\pm 0.05 \pm 0.15\tau$). MODIS/AERONET τ regression has an equation of: y = 1.01x + 0.03, R = 0.90. Global (the 6300 granules) mean τ has been reduced from 0.28 to 0.21. Retrievals of η show less significant improvement, but are still better correlated with AERONET results than previous versions. Retrievals of spectral Ångstrom Exponent show little or no improvement at this time. However, the new algorithm's derivation of Fine τ (τ x η) is much improved. This product that can be related to the anthropogenic contribution to the total τ (e.g. Kaufman et al., 2005) and has specific applications for the air quality community. Finally, the V5.2 products' quality assurance (QA) has been overhauled and is now more useful to users within the aerosol community.

References

Anderson, T.L., Y. Wu, D.A. Chu, B.Schmid, J. Redemann and O. Dubovik (2006), Testing the MODIS satellite retrieval of aerosol fine-mode fraction, *J.Geophys.Res.*, *110*(D18204), doi: 10.1029/2005JD005978.

Al-Saadi, J., J. Szykman, R. B. Pierce, C. Kittaka, D. Neil, D. A. Chu, L. Remer, L. Gumley, E. Prins, L. Weinstock, C. MacDonald, R. Wayland, F. Dimmick, and J. Fishman (2005), Improving National Air Quality Forecasts with Satellite Aerosol Observations. *Bull. Am. Met. Soc.*, *86* (9), 1249-1261.

Bodhaine, B. A., N. B. Wood, et al. (1999), On Rayleigh optical depth calculations, *J. Atmos. Ocean. Tech. 16*(11), 1854-1861.

Chu, D. A., Y. J. Kaufman, et al. (2002), Validation of MODIS aerosol optical depth retrieval over land, *Geophys, Res. Lett. 29*(12): art. no.-1617.

Chu, D. A., L. A. Remer, Y. J. Kaufman, B. Schmid, J. Redemann, K. Knobelspiesse, J. D. Chern, J. Livingston, P. B. Russell, X. Xiong, and W. Ridgway (2005), Evaluation of aerosol properties over ocean from Moderate Resolution Imaging Spectroradiometer (MODIS) during ACE-Asia. *J. Geophys. Res.*, *110* (D07308), doi: 10.1029/2004/JD005208.

Chu, D. A., Y. J. Kaufman, G. Zibordi, J. D. Chern, J. Mao, C. Li, and B. N. Holben, (2003), Global monitoring of air pollution over land from EOS- Terra MODIS, *J. Geophys. Res, 108* (D21), 4661, doi: 10.1029/2002JD003179.

Dubovik, O., B. N. Holben, et al. (2002), Non-spherical aerosol retrieval method employing light scattering by spheroids, *Geophys, Res. Lett. 29*(10): art. no.-1415.

Dubovik, O. and M. D. King (2000), A flexible inversion algorithm for retrieval of aerosol optical properties from Sun and sky radiance measurements, *J. Geophys. Res, 105*(D16), 20673-20696.

Dubovik, O., A. Sinyuk, T. Lapyonok, B. N. Holben, M. Mishchenko, P. Yang, T. F. Eck, H. Volten, O. Munoz, B. Veihelmann, van der Zander, M Sorokin, and I. Slutsker, (2006) Application of light scattering by spheroids for accounting for particle non-sphericity in remote sensing of desert dust, *J. Geophys. Res.*, *111*(D11208), doi: 10.1029/2005JD006619.

Eck, T. F., B. N. Holben, et al. (1999), Wavelength dependence of the optical depth of biomass burning, urban, and desert dust aerosols, *J. Geophys. Res, 104*(D24), 31333-31349.

Evans, K.F. and G. L. Stephens, 1991, A New Polarized Atmospheric Radiative Transfer Model, *J. Quant. Spectrosc. Radiat. Transfer, 46*(5), 413-423.

Fraser, R. H., Ferrare, R. A., Kaufman, Y. J., Mattoo, S. (1989). Algorithm for Atmospheric Corrections of Aircraft and Satellite Imagery. <u>NASA Technical Memorandum 100751</u>. Greenbelt, MD USA, NASA Goddard Space Flight Center.

Gatebe, C. K., M. D. King, et al. (2001). Sensitivity of off-nadir zenith angles to correlation between visible and near-infrared reflectance for use in remote sensing of aerosol over land, *IEEE Trans. Geosci. Remote Sens. 39*(4), 805-819.

Holben, B. N., T. F. Eck, et al. (1998), AERONET - A federated instrument network and data archive for aerosol characterization, *Remote Sens. Environ. 66*(1), 1-16.

Ichoku, C., L. A. Remer, et al. (2003), MODIS observation of aerosols and estimation of aerosol radiative forcing over southern Africa during SAFARI 2000, *J. Geophys. Res, 108*(D13), 8499, doi: 10.1029/2002JD002366.

Ichoku, C., D. A. Chu, et al. (2002), A spatio-temporal approach for global validation and analysis of MODIS aerosol products, *Geophys, Res. Lett. 29*(12): art. no.-1616.

Intergovernmental Panel on Climate Change (IPCC), 2001, <u>Climate Change 2001: The Scientific Basis</u>, J. T. Houghton, Y. Ding, D.J. Griggs, M. Noguer, P. J. van der Linden and D. Xiaosu (Eds.), Cambridge University Press, UK. pp 944.

Kaufman, Y. J., O. Boucher, et al. (2005), Aerosol anthropogenic component estimated from satellite data, *Geophys, Res. Lett. 32*(17).

Kaufman, Y. J., N. Gobron, et al. (2002), Relationship between surface reflectance in the visible and mid-IR used in MODIS aerosol algorithm – theory, *Geophys, Res. Lett. 29*(23), art. no.-2116.

Kaufman, Y. J., D. Tanré, et al. (1997a), Operational remote sensing of tropospheric aerosol over land from EOS moderate resolution imaging spectroradiometer. *J. Geophys. Res, 102*(D14), 17051-17067.

Kaufman, Y. J., A. E. Wald, et al. (1997b). "The MODIS 2.1-μm channel - Correlation

with visible reflectance for use in remote sensing of aerosol." *IEEE Trans. Geosci. Remote Sens. 35*(5), 1286-1298.

Kaufman, Y. J., and C. Sendra, (1988), Algorithm for atmospheric corrections of visible and Near IR satellite imagery, *Int. J. Rem. Sens., 9*, 1357-1381.

King, M. D., W. P. Menzel, Y. J. Kaufman, D. Tanre, B.-C. Gao, S. Platnick, S. A. Ackerman, L. A. Remer, R. Pincus, and P. A. Hubanks (2003), Cloud and aerosol properties, precipitable water, and profiles of temperature and humidity from MODIS. *IEEE Trans. Geosci. Remote Sens., 41*, 442-458.

Kleidman, R. G., N. T. O'Neill, et al. (2005), Comparison of moderate resolution Imaging spectroradiometer (MODIS) and aerosol robotic network (AERONET) remote-sensing retrievals of aerosol fine mode fraction over ocean, *J. Geophys. Res, 110*(D22), Art. No. D22205.

Levy, R. C., L. A. Remer, et al. (2004), Effects of neglecting polarization on the MODIS aerosol retrieval over land, *IEEE Trans. Geosci. Remote Sens 42*(11), 2576-2583.

Levy, R. C., L. A. Remer, et al. (2005), Evaluation of the MODIS aerosol retrievals over ocean and land during CLAMS, *J. Atmos. Sci., 62*(4), 974-992.

Levy, R.C., L.A. Remer and O. Dubovik et al. (2006), Aerosol optical properties and lookup tables for the new MODIS aerosol retrieval over land, submitted to JGR.

Levy, R.C., L.A. Remer, S. Mattoo, E. Vermote, Y.J. Kaufman, (2006), A new algorithm for retrieving aerosol properties over land from MODIS spectral reflectance, submitted to JGR.

Li, R. R., L. Remer, et al. (2005). Snow and ice mask for the MODIS aerosol products." *IEEE Geo. and Rem. Sens. Lett., 2*(3), 306-310.

Lyapustin, A. I. (2001), Three-dimensional effects in the remote sensing of surface albedo, *IEEE Trans. Geosci. Remote Sens 39*(2), 254-263.

Martins, J. V., D. Tanré, et al. (2002), MODIS Cloud screening for remote sensing of aerosols over oceans using spatial variability, *Geophys, Res. Lett., 29*(12), doi: 10.1029/2001GL01352.

O'Neill, N. T., Eck, T. F., Smirnov, A., Holben, B. N. and Thulasiraman, S. (2003), Spectral discrimination of coarse and fine mode optical depth., *J Geophys. Res., 108*, doi:10.1029/2002JD002975.

O'Neill, N. T., Smirnov, A., Holben, B., and Thulasiraman, S. (2005), Spectral Deconvolution algorithm: Technical memo.

Omar, A. H., J. G. Won, et al. (2005), Development of global aerosol models using cluster analysis of Aerosol Robotic Network (AERONET) measurements, *J Geophys. Res., 110*(D10).

Remer, L. A. and Y. J. Kaufman (1998), Dynamic aerosol model: Urban/industrial aerosol, *J Geophys. Res., 103*(D12), 13859-13871.

Remer, L. A., Y. J. Kaufman, et al. (2005). "The MODIS aerosol algorithm, products, and validation *J. Atmos. Sci., 62*(4), 947-973.

Remer, L. A., A. E. Wald, et al. (2001), Angular and seasonal variation of spectral surface reflectance ratios: Implications for the remote sensing of aerosol over land, *IEEE Trans. Geosci. Remote Sens., 39*(2), 275-283.

Tanré, D., Y. J. Kaufman, et al. (1997), Remote sensing of aerosol properties over oceans using the MODIS/EOS spectral radiances, *J Geophys. Res., 102*(D14), 16971-16988.

Tucker, C. J. (1979), Red and photographic infrared linear combinations monitoring vegetation, *Remote Sens. Environ., 8*, 127-150.

U.S. Government Printing Office, (1976), U.S. Standard Atmosphere, Washington, D.C.

Vermote, E. F., D. Tanré, et al. (1997), Second Simulation of the Satellite Signal in the Solar Spectrum, 6S: An overview, *IEEE Trans. Geosci. Remote Sens., 35*(3), 675-686.

Wiscombe, W. J. (1981), Improved Mie scattering algorithms, *Appl. Opt., 19*, 1505-1509.

Yu, H., Y. J. Kaufman, M. Chin, G. Feingold, L. Remer, T. Anderson, Y. Balkanski, N. Bellouin, O. Boucher, S. Christopher, P. DeCola, R. Kahn, D. Koch, N. Loeb, M. S. Reddy, M. Schulz, T. Takemura, and M. Zhou (2006), A review of measurement-based assessments of aerosol direct radiative effect and forcing, *Atmos. Chem . Phys., 6*, 613-666.

TABLE 2: SOLAR/SURFACE/SATELLITE GEOMETRY FOR EIGHT EXAMPLES

Reference	Solar Zenith	View Zenith	Relative Azimuth	Scattering Angle
A	12.00	6.97	60.00	163.40
B	12.00	52.84	60.00	120.53
C	12.00	6.97	120.00	169.59
D	12.00	52.84	120.00	132.35
E	36.00	6.97	60.00	140.12
F	36.00	52.84	60.00	104.74
G	36.00	6.97	120.00	147.00
H	36.00	52.84	120.00	136.29

All units are degrees

TABLE 1: LIST OF PRESCRIBED ERRORS FOR V5.2 SENSITIVITY STUDY

Reference	Error Name	Description
1	LUTinput	LUT input: Use the LUT with no prescribed errors
2	ModError	Aerosol model error: We tried to retrieve with the Non-absorbing fine model LUT
3	RndError	Random Error: All channels have random reflectance error of up to ±0.002
4	SfcError	Surface Error: 10% error in assumed 0.66/2.12 surface reflectance relationship
5	CalError	Calibration Error: All channels have random error of up to ±1%
6	ElvError	Elevation Error: Elevation is 1km instead of assumed sea level
7	GeoError	Geometry Error: All angles have random error of up to ±5 degrees
8	AllError	Combination of 2,3,4,5,6 and 7.

Geometry Error Name	LUTinput	RndError	CalError	GeoError	ModError	ElvError	SfcError	AllError
A	0.501	0.4786	0.5242	0.5143	0.5015	0.6068	0.5402	0.6963
B	0.501	0.4887	0.5242	0.4977	0.4993	0.6035	0.5422	0.6677
C	0.501	0.5227	0.5227	0.4657	0.4835	0.5104	0.4955	0.4809
D	0.5011	0.5104	0.4995	0.4761	0.5014	0.5228	0.498	0.4892
E	0.5008	0.4754	0.502	0.4893	0.4866	0.5211	0.4877	0.5737
F	0.501	0.5135	0.5029	0.4922	0.5035	0.531	0.488	0.5536
G	0.5014	0.4973	0.5199	0.4698	0.4811	0.5097	0.488	0.427
H	0.5016	0.4961	0.5001	0.4744	0.5198	0.5299	0.4939	0.5106

A: Retrieved τ at 0.55 μm (expected τ=0.5)

Product Error Name	LUTinput	RndError	CalError	GeoError	ModError	ElvError	SfcError	AllError
τ	0.0011(+)	0.0159	0.0162	0.0215	0.0123	0.0561(+)	0.0221	0.1006
η	0.0000	0.0000	0.0707	0.1000	0.0707	0.4243 (+)	0.1323 (+)	0.4912 (+)
ρ	0.0004 (-)	0.0008	0.0022	0.0025	0.0031 (-)	0.0067	0.0020 (+)	0.0074 (+)
ϵ	0.0010	0.0021	0.0037	0.0028	0.0020	0.0025	0.0035	0.0052

B: MSE of retrieved $\tau, \eta, \rho^{\sigma}$ and ϵ (expected τ=0.5, η=0.5, ρ^{σ}=0.15 and ϵ=0.0). Entries designated with (+) mean that the product was over-estimated for all 8 geometries, whereas those with a (-) means it was under-estimated for all geometries.

TABLE 4: CONTENTS OF MODIS V5.2 AEROSOL LEVEL 2 FILE (MOD04/MYD04): LAND PRODUCTS

Name of Product (SDS)	Dimesions: 3rd Dimension	Type of product
Corrected_Optical_Depth_Land	X,Y,3: 0.47, 0.55, 0.66 μm	Retrieved Primary
Corrected_Optical_Depth_Land_wav2p1	X,Y,1: 2.12 μm	Retrieved Primary
Optical_Depth_Ratio_Small_Land	X,Y: (for 0.55 μm)	Retrieved Primary
Surface_Reflectance_Land	X,Y,3: 0.47, 0.66, 2.12 μm	Retrieved Primary
Fitting_Error_Land	X,Y: (at 0.66 μm)	Retrieved By-Product
Quality_Assurance_Land	X,Y,5: 5 bytes	Diagnostic
Aerosol_Type_Land	X,Y:	Diagnostic
Angstrom_Exponent_Land	X,Y: (for 0.66/0.47 μm)	Derived
Mass_Concentration_Land	X,Y:	Derived
Optical_Depth_Small_Land	X,Y,4: 0.47,0.55,0.66,2.12 μm	Derived
Mean_Reflectance_Land	X,Y,7: 0.47,0.55,0.66,0.86,1.2,1.6,2.12μm	Diagnostic
STD_Reflectance_Land	X,Y,7: 0.47,0.55,0.66,0.86,1.2,1.6,2.12μm	Diagnostic
Cloud_Fraction_Land	X,Y:	Diagnostic
Number_Pixels_Used_Land	X,Y:	Diagnostic
Path_Radiance_Land	X,Y,2: 0.47, 0.66 μm	Experimental
Error_Path_Radiance_Land	X,Y,2: 0.47, 0.66 μm	Experimental
Critical_Reflectance_Land	X,Y,2: 0.47, 0.66 μm	Experimental
Error_Crit_Reflectance_land	X,Y,2: 0.47, 0.66 μm	Experimental
Error_Critical_Reflectance_Land	X,Y,2: 0.47, 0.66 μm	Experimental
Quality_Weight_Path_Radiance_Land	X,Y,2: 0.47, 0.66 μm	Experimental
Quality_Weight_Crit_Reflectance_Land	X,Y,2: 0.47, 0.66 μm	Experimental
Optical_Depth_Land_And_Ocean	X,Y: 0.55 μm	Joint Land and Ocean
Image_Optical_Depth_Land_And_Ocean	X,Y: 0.55 μm	Joint Land and Ocean
Optical_Depth_Ratio_Small_Land_And_Ocean	X,Y: 0.55 μm	Joint Land and Ocean

X = 135; Y = 203. If there is a 3rd dimension of the SDS, then the indices of it are given. The "Retrieved" parameters are the solution to the inversion, whereas "Derived" parameters follow from the choice of solution. "Diagnostic" parameters aid in understanding of the directly Retrieved or Derived products. "Experimental" products are unrelated to the inversion but may have future applications. "Joint Land and Ocean" indicate combined land and ocean products.

TABLE 5: DESCRIPTION OF DATA USED IN V5.2 PROVISIONAL VALIDATION

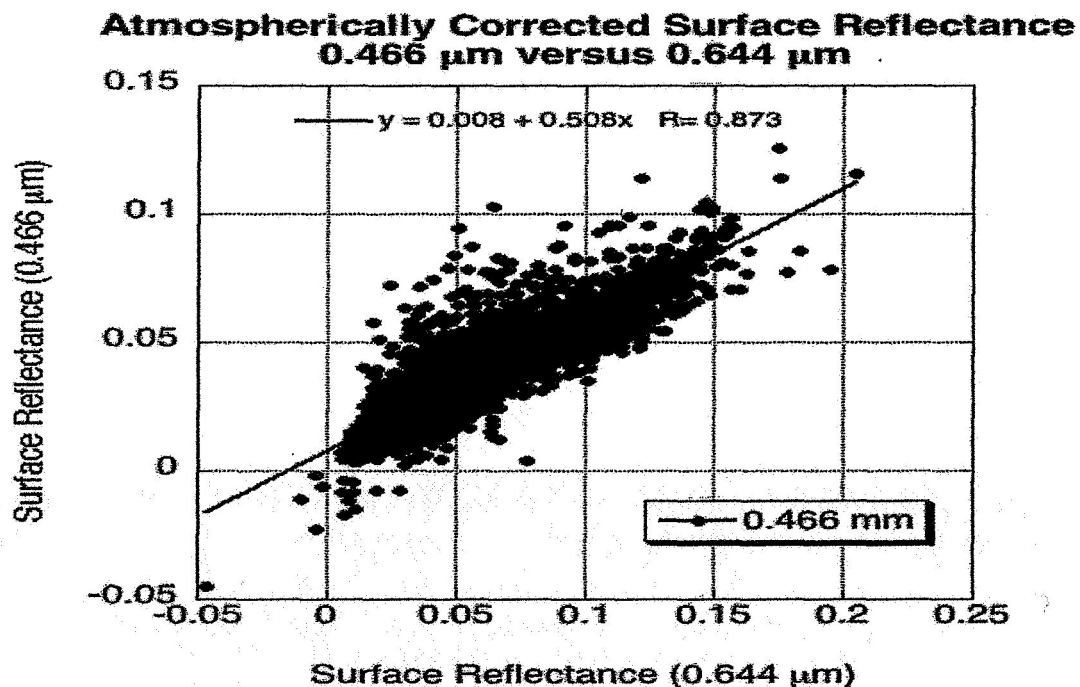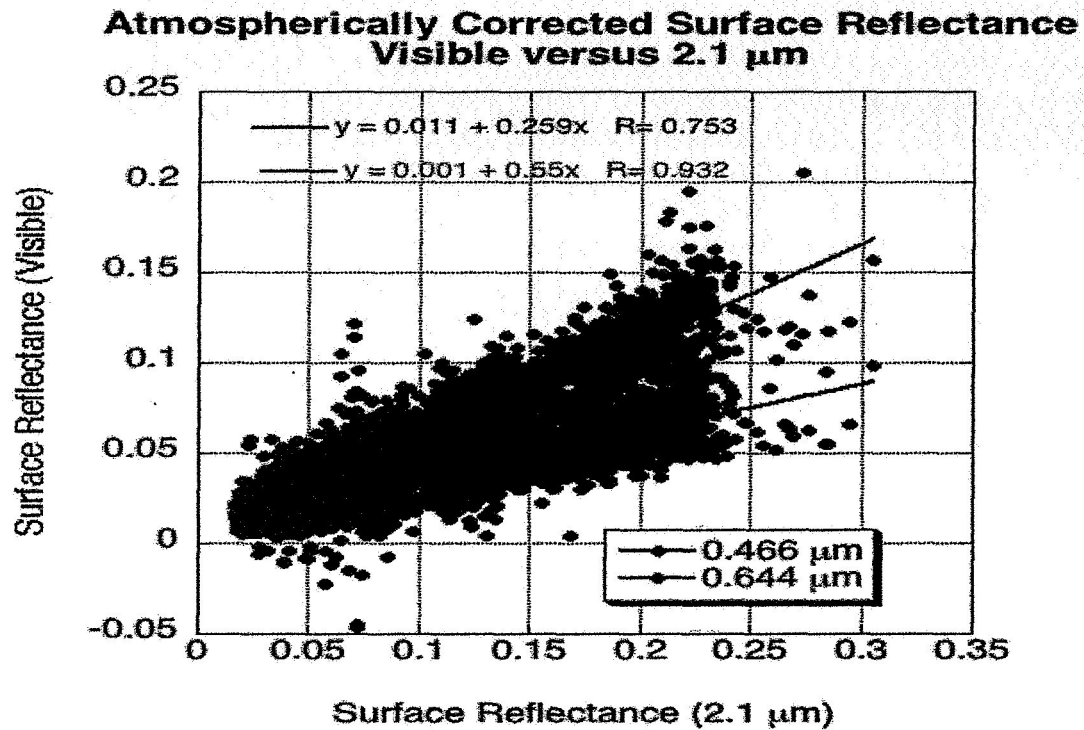| Date of MODIS Observations	Terra/Aqua	Why interesting?
August 2001 (full month: 4138 granules)	Terra and Aqua	
7 July 2002 (full day: 132 granules)	Aqua	Quebec Smoke in NE US
8 July 2002 (full day: 136 granules)	Aqua	Quebec Smoke in NE US
6 Mar 2004 (full day: 132 granules)	Aqua	Asian Dust
7 Mar 2004 (full day: 138 granules)	Aqua	Asian Dust
Eight days in 2003 (full days: 1070 granules)	Aqua	Yearly Cycle
14 Nov 2005 (full day: 138 granules)	Terra	Low AOD globally
22 Apr 2001 (full day: 136 granules)	Terra	ACE-Asia
26 Jun 2002 (full day: 138 granules)	Terra	Summer time haze
Test_bed_Aqua: (39 granules)	Aqua	Test bed of interesting Aqua data
Test_bed_Terra: (102 granules)	Terra	Test bed of interesting Terra data

Total granules = 6299

39

Figure 1: Atmospherically corrected surface reflectance in the visible (0.47 and 0.66 μm channels) compared with that in the 2.12 μm SWIR channel (a), and the 0.47μm compared with that in the 0.66 μm channel (b).

Figure 2: VIS/SWIR surface reflectance relationships as a function of scattering angle. The data were sorted according to scattering angle and put into 20 groups of equal size (about 230 points for each scattering angle bin). On all subplots, each point is plotted for the median value of scattering angle in the bin. Part (a) plots median values of reflectance at each channel as a function of the scattering angle. Linear regression was calculated for the 230 points in each group. The slope of the regression (for each angle bin) is plotted in (b), the y-intercept is plotted in (c) and the regression correlation is plotted in (d). Note for (b), (c) and (d) that 0.47 μm vs 2.12 μm (r0470) is plotted in blue, 0.66 μm vs 2.12 μm (r0660) is plotted in red and 0.47 vs 0.66 μm (rvis) is plotted in green.

Figure 3: 0.66 μm versus 2.12 μm surface reflectance as a function of bins of *NDVI_SWIR* values. The standard regression is plotted, with regression equations given in the lower right hand corner. The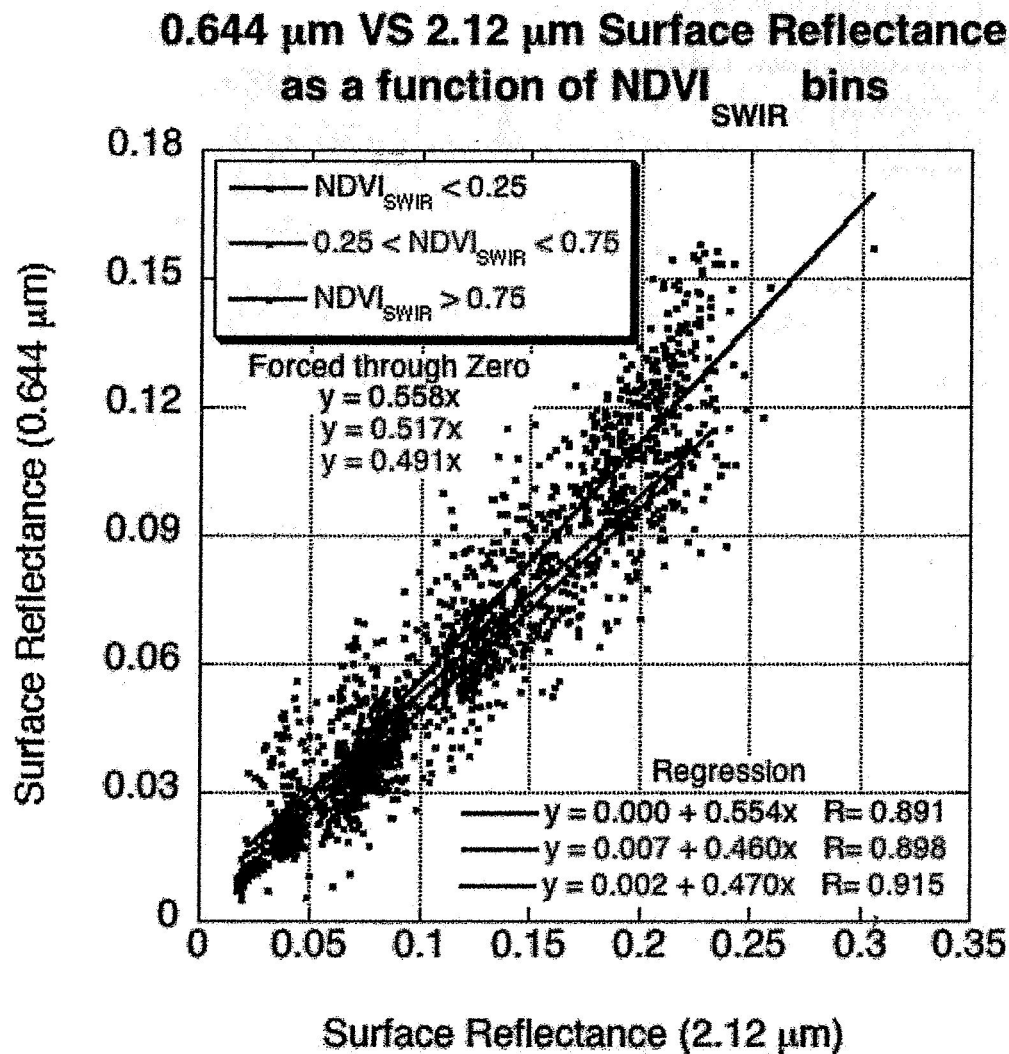 ratios (if forced through zero) are given beneath the legend. Blue refers to low *NDVI_SWIR*, red to medium and green to high values.

MODIS Over Land Algorithm
All procedures applied to individual boxes of 20 x 20 pixels at 500 m resolution (10 km at nadir)

•Ensure angles and reflectance values are valid. If not, report Fill values and EXIT
•Identify and mask (discard) all water, cloudy and snow/ice pixels.
•Identify "dark target pixels" that have $0.01 \le \rho_{2.13} \le 0.25$
•Discard brightest 50% and darkest 20% of pixels defined with $\rho_{0.66}$
... leaving a maximum of 120 pixels

Are there at least 12 (10%) dark target pixels?

yes   no

Procedure A
Set QAC=0,1,2 or 3 (based on # of pixels)

•For all identified 'dark' pixels,
  Calculate mean $\rho_{0.47}$, $\rho_{0.66}$, $\rho_{2.1}$, $\rho_{1.2}$
  Calculate NDVI$_{SWIR}(\rho_{2.1}, \rho_{1.2})$
•Assume surface reflectance relationships:
  $\rho'_{0.66} = f(\rho'_{2.12}, NDVI_{SWIR}, \Theta); \rho'_{0.47} = g(\rho'_{0.66}, \Theta)$
•Select fine model aerosol type LUT
  (function of geography and season)
•Select coarse model aerosol LUT (dust)
•Correct lookup tables for elevation
•Interpolate lookup tables on geometry

Do Inversion

For 13 values of η
  (-0.1,0.0,0.1,...0.9,1.0,1.1)...
Find $\tau_{0.55}$ and $\rho^s_{2.1}$ such that
  $\rho^{MODIS}_{0.47} - \rho^{TOA}_{0.47} = 0$,
where $\rho^{TOA}_\lambda = \eta(\rho^{fine}_\lambda) + (1-\eta)(\rho^{coarse}_\lambda)$
Choose η such that
  $\rho^{MODIS}_{0.66} - \rho^{TOA}_{0.66} = \varepsilon$ is minimized

Primary products: $\tau_{0.55}$, η, $\rho^s_{2.1}$, ε

•Calculate τ_λ, ρ^s_λ, α, M_C, τ^{fine}_λ
•If $\eta=-0.1$ set $\eta=0.0$; If $\eta=1.1$ set $\eta=1.0$
•If $\tau_{0.55} < 0.2$, then set η = Fill
•If $\varepsilon > 0.25$, then set QAC = 0

Procedure B
Set QAC=0
Identify and count pixels where
$\rho_{2.13} > 0.25$ and $\rho_{2.13} \le 0.25$ G(μ,μ_o) <0.40

yes   **Is N $\ge$ 12?**   no   Report Fill values & error codes   EXIT

•Assume surface reflectance relationships:
  $\rho'_{0.66} = f(\rho'_{2.12}, NDVI_{SWIR}, \Theta); \rho'_{0.47} = g(\rho'_{0.66}, \Theta)$
•Assume Continental aerosol model (only)
•Correct lookup table for elevation
•Interpolate lookup table on geometry

Do Single Channel Retrieval

Find $\tau_{0.55}$ and $\rho^s_{2.1}$ such that
  $\rho^{MODIS}_{0.47} - \rho^{TOA}_{0.47} = 0$,
where $\rho^{TOA}_\lambda = \rho^{Continental}_\lambda$

Primary products: $\tau_{0.55}$, $\rho^s_{2.1}$

•Calculate $\tau_{0.47}$, M_C
•Set η, $\tau_{0.66}$, $\tau_{2.1}$, α, τ^{fine}_λ = Fill

If $\tau_{0.55} \le 0.0$ then set α=Fill, M_C=0, τ^{fine}_λ=0
If $-0.1 < \tau_{0.55} \le -0.05$, then set $\tau_\lambda = -0.05$
If $\tau_{0.55} \le -0.10$, then set τ_λ, α, M_C, τ^{fine}_λ = Fill

Is $\tau_{0.55} < 0.0$?   yes   no   Report: τ_λ, ρ^s_λ, α, M_C, τ^{fine}_λ, QA, etc   **EXIT**
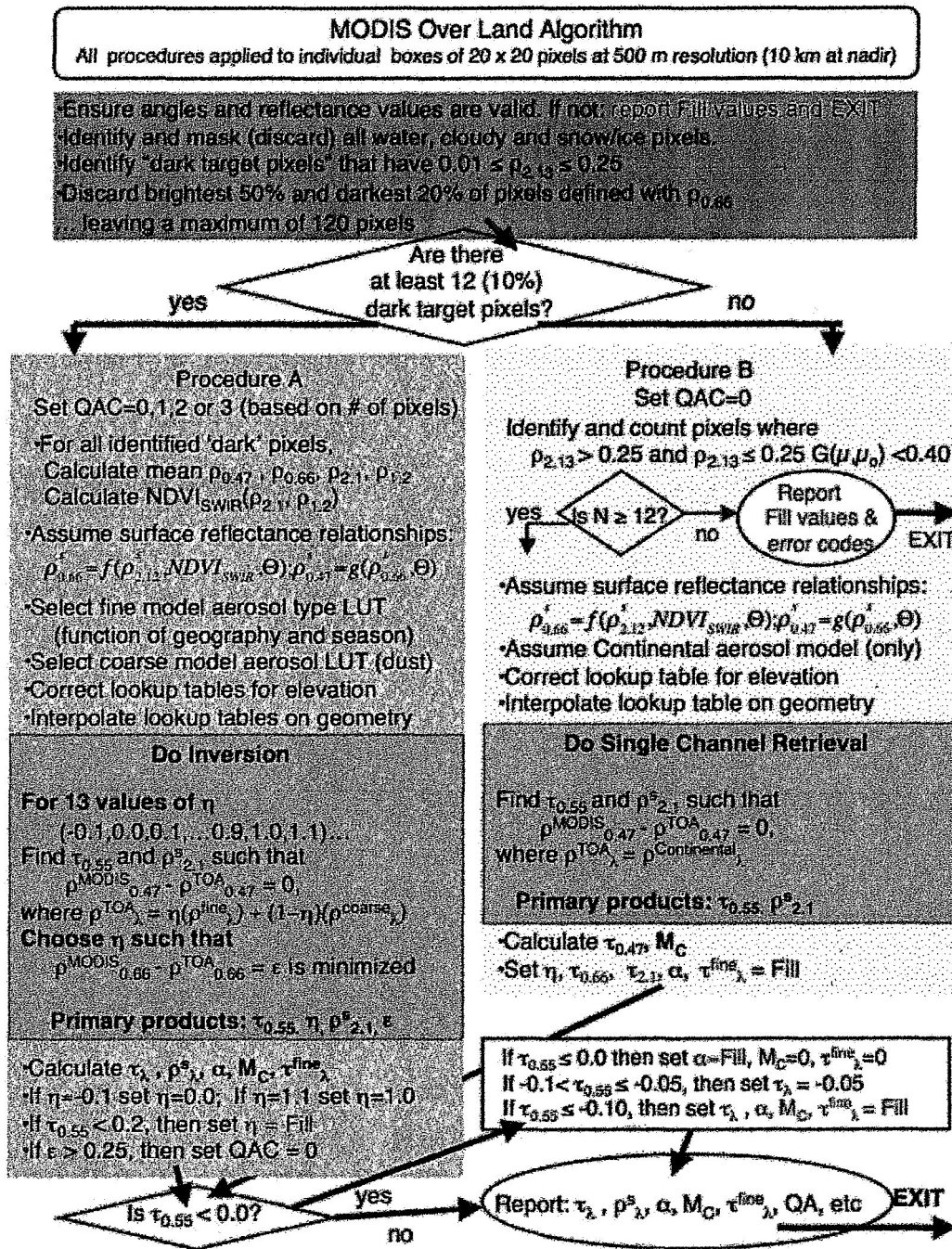
Figure 4: Flowchart illustrating the derivation of aerosol over land for V5.2.
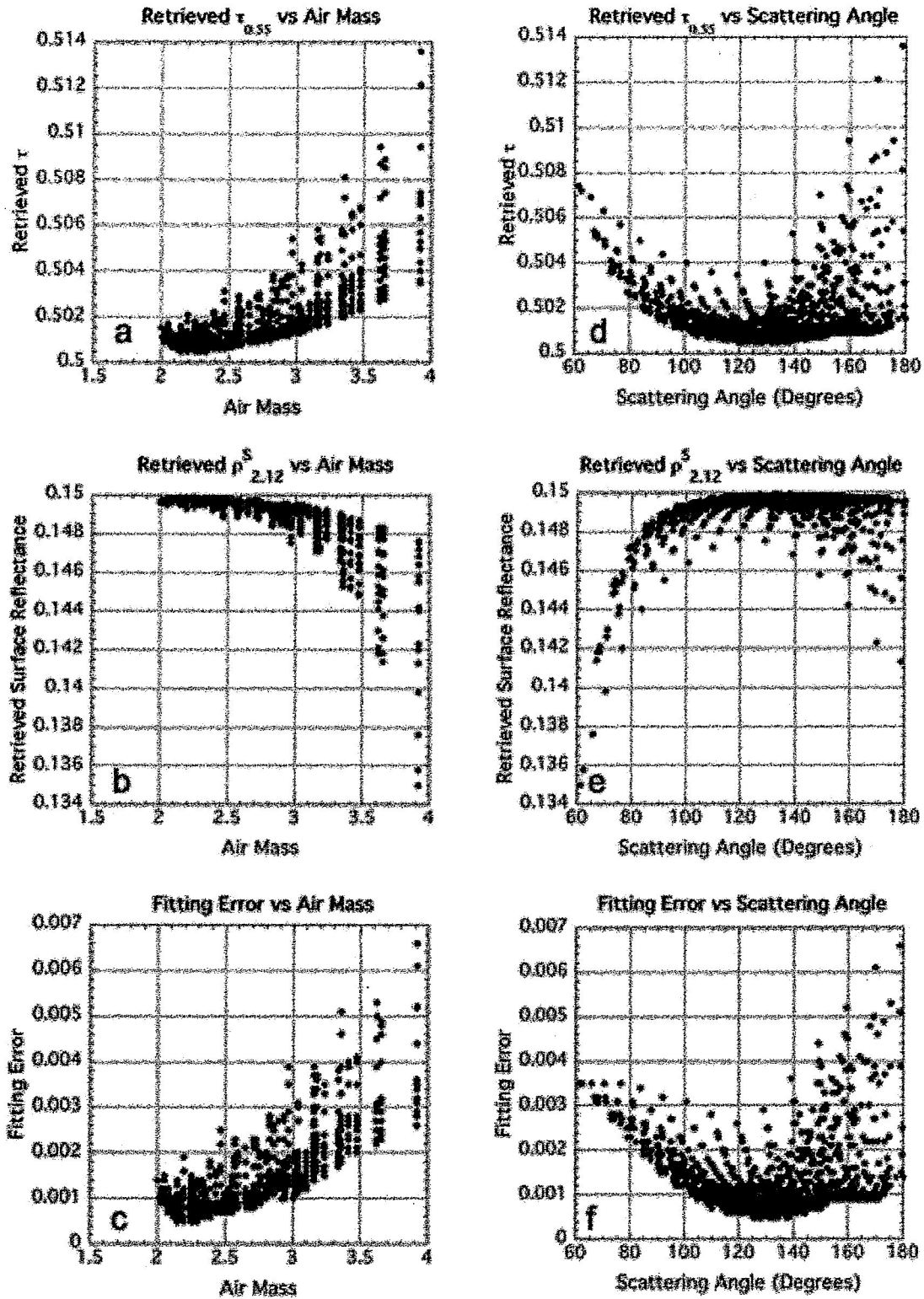
44

Figure 5: Retrieved MODIS products as a function of Air Mass (a-c) and Scattering Angle (d-f) for inputted atmospheric conditions (τ=0.5, η=0.5 and $\rho^s_{2.12}$=0.15) and 720 LUT geometrical combinations. The retrieved τ is plotted in (a) and (d), the 2.12

μm surface reflectance in (b) and (e) and the fitting error is plotted in (c) and (f). Note that in all cases, the η value of 0.5 was retrieved exactly.
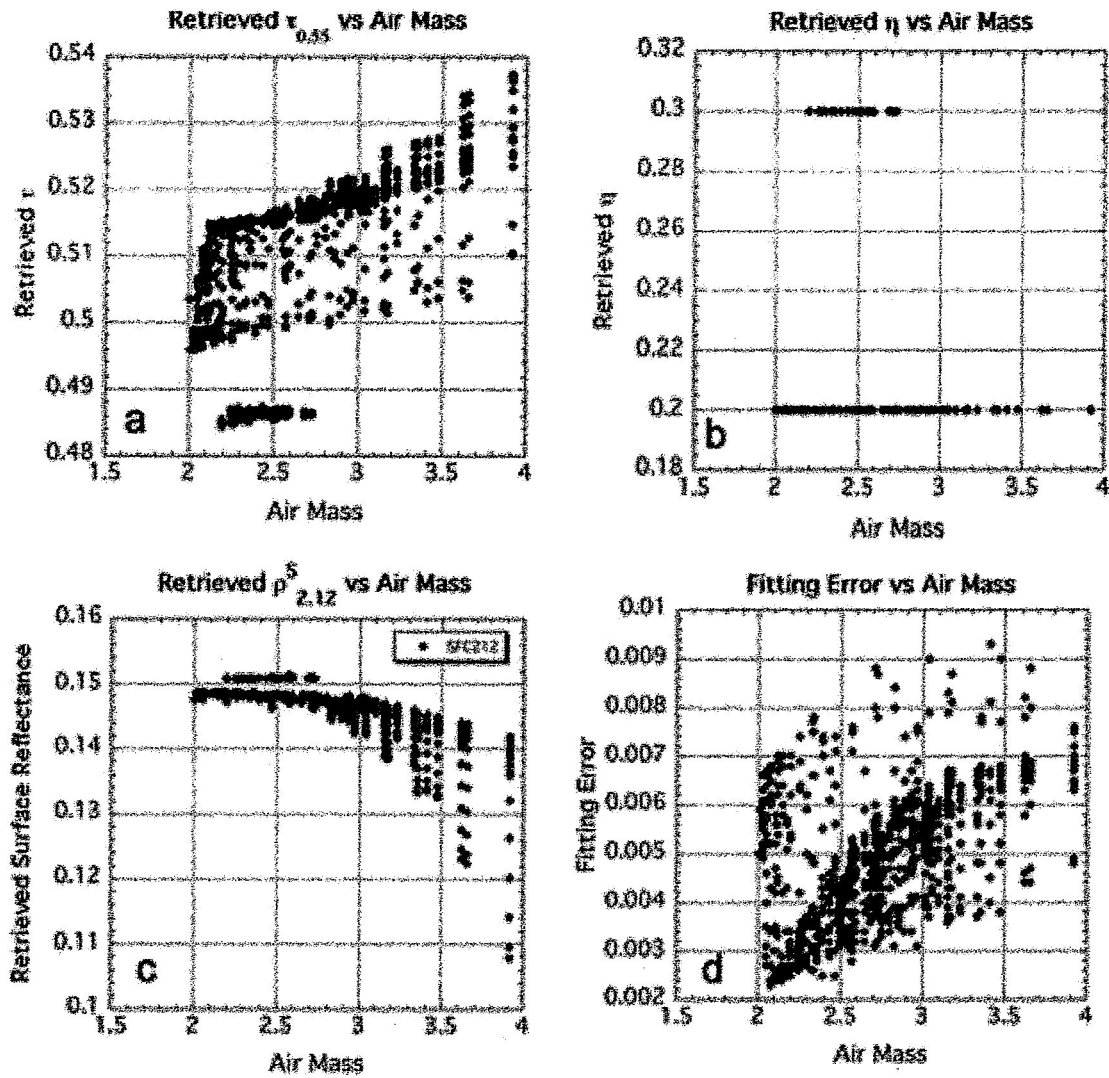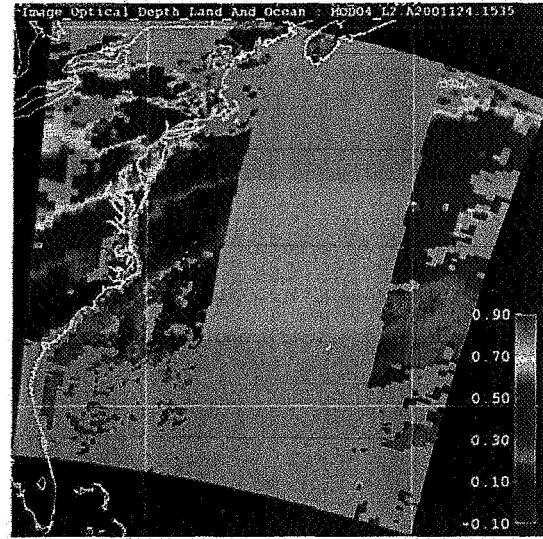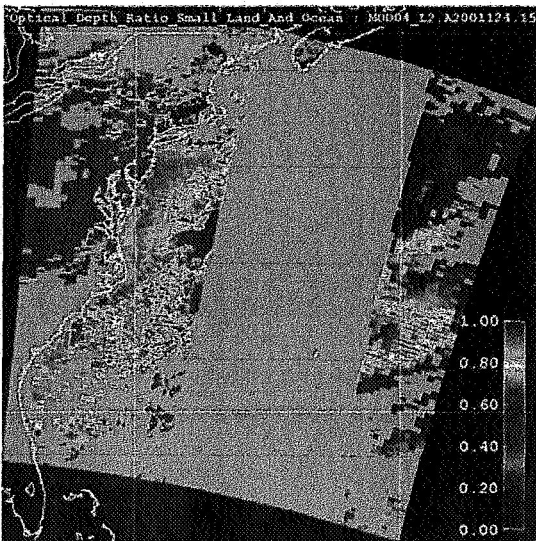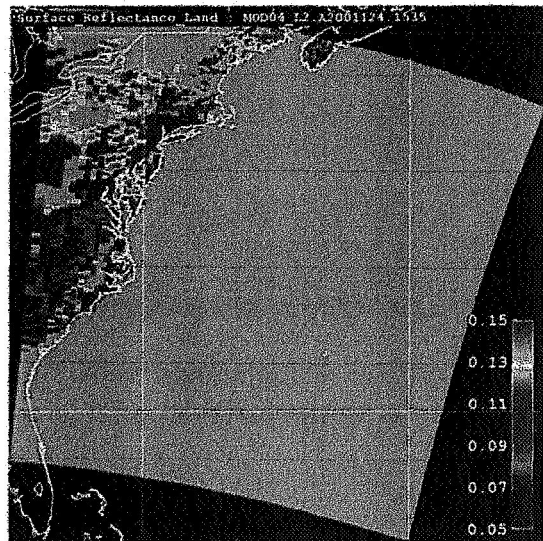
Figure 6: Retrieved MODIS products as a function of Air Mass for inputted atmospheric conditions ($\tau=0.5$, $\eta=0.25$ and $\rho^s_{2.12}=0.15$) and 720 LUT geometrical combinations. The retrieved τ is plotted in (a), retrieved η in (c), the 2.12 μm surface reflectance in (c) and the fitting error is plotted in (d).

A) RGB: ρ^M(0.66,0.55,0.47 μm)

B) τ(0.55 μm)

C) η(0.55 μm)

D) ρ^s (2.1 μm)

Figure 7: Retrieved aerosol and surface properties over the Eastern U.S. on May 4, 2001. This figure can be compared with that plotted in King et al., (2003). Panel A) is a 'true-color' composite image of three visible channels, showing haze over the mid-Atlantic. Panels B) and C) show retrieved τ and η, showing that the heavy aerosol ($\tau \sim 1.0$) is dominated by fine particles. The transport of the aerosol into the Atlantic is well represented with good agreement between land and ocean. In fact the continuity of τ seems to be improved since earlier versions of the aerosol algorithm. Note that over-land η is not reported when $\tau < 0.2$. Panel D) shows the retrieved surface reflectance.

48

Sep 30, 2003; 17:55 UTC

OLD: AOT at 0.55μm

NEW: AOT at 0.55μm
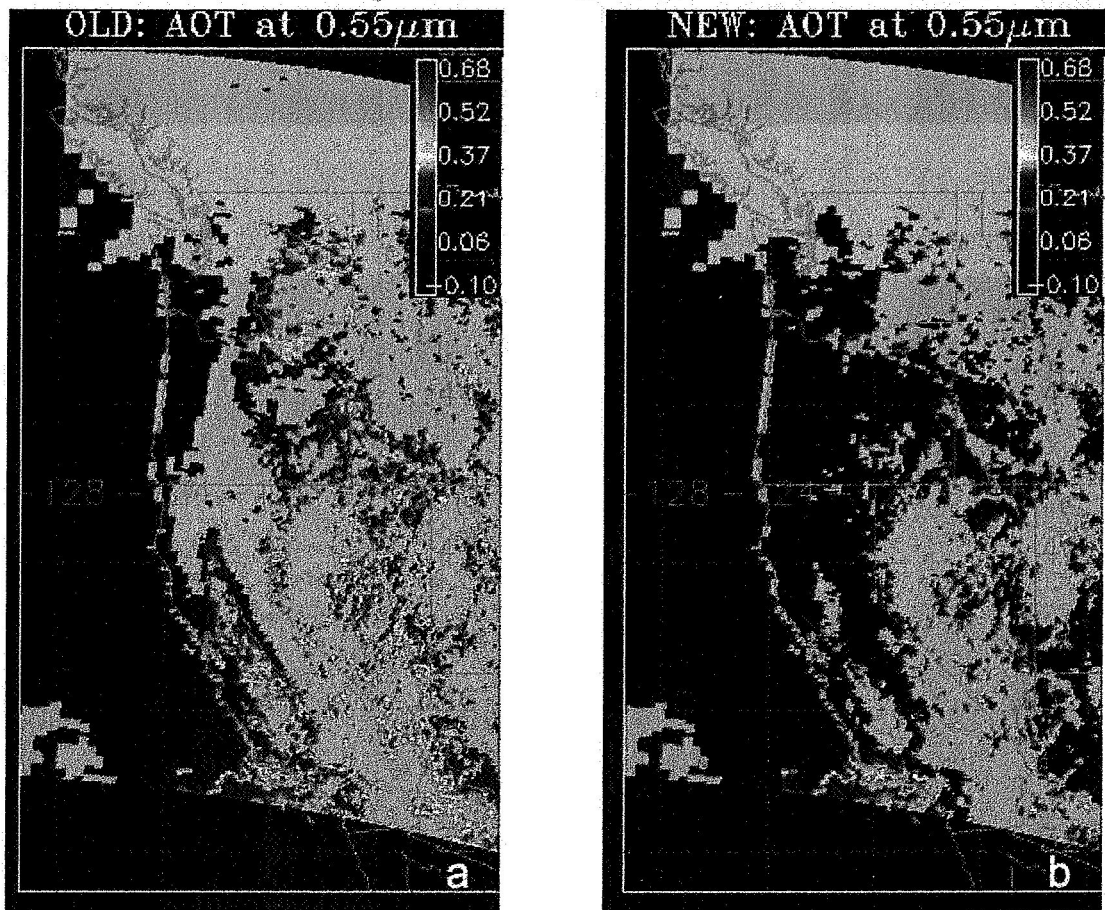
0.68
0.52
0.37
0.21
0.08
-0.10

a

b

Figure 8: Retrieved τ (AOT) at 0.55 μm for Old V5.1 (a) and New V5.2 (b) over California for 30 September 2003. The color scale is the same for both plots. Note the increase in the retrieval spatial coverage and reduction in surface contamination for V5.2.
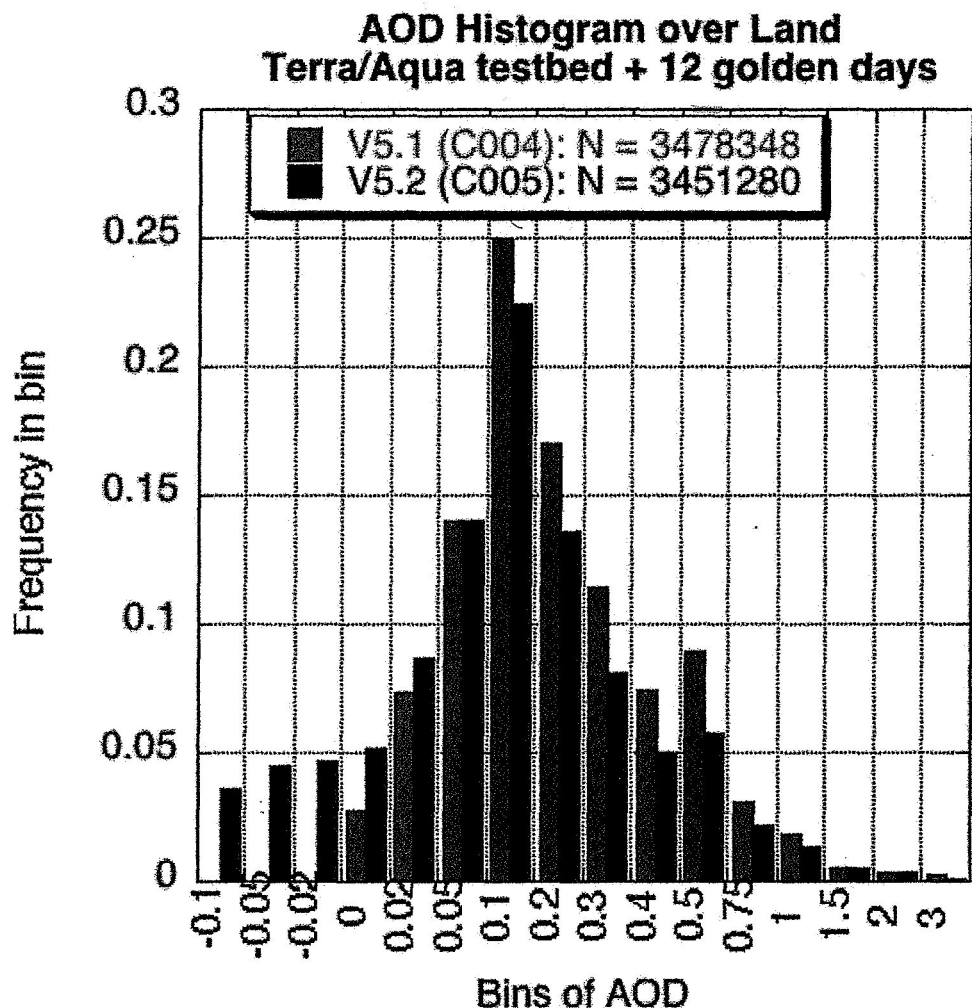
AOD Histogram over Land
Terra/Aqua testbed + 12 golden days

Legend:
- V5.1 (C004): N = 3478348
- V5.2 (C005): N = 3451280

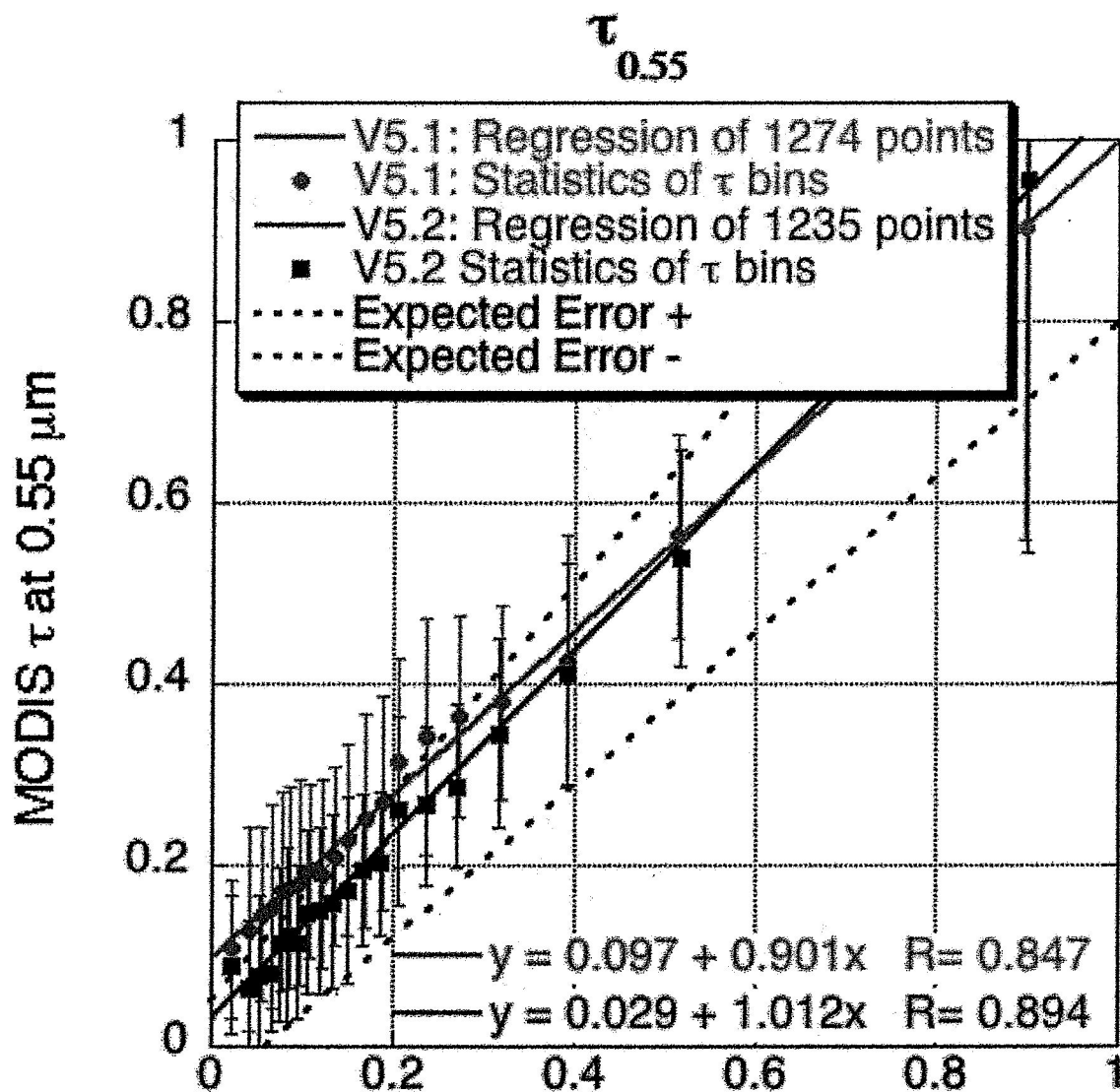Y-axis: Frequency in bin
X-axis: Bins of AOD

Figure 9: Histogram of retrieved τ (AOD) over land, from V5.2 (C005) in green, compared to V5.1 (C004) in orange. The data include the 141 granules of the Terra and Aqua "test_bed" as well as twelve complete days. The value of each bin refers to the minimum value of the bin (the max value would be the value of the next bin). Note that the general lognormal nature of the retrievals is preserved, except now there are some negative values.

Figure 10: MODIS τ over land retrieved at 0.55 μm, compared with AERONET τ interpolated to 0.55 μm. The solid shapes and error bars represent the mean and standard deviation of the MODIS retrievals, in 20 bins of AERONET-derived τ. Both the retrievals from V5.1 (orange) and V5.2 (green) are shown. The regressions (solid lines) are for the cloud of all points before binning (not shown). The expected errors for MODIS (±0.05 ±0.15τ) are also shown (dashed lines).
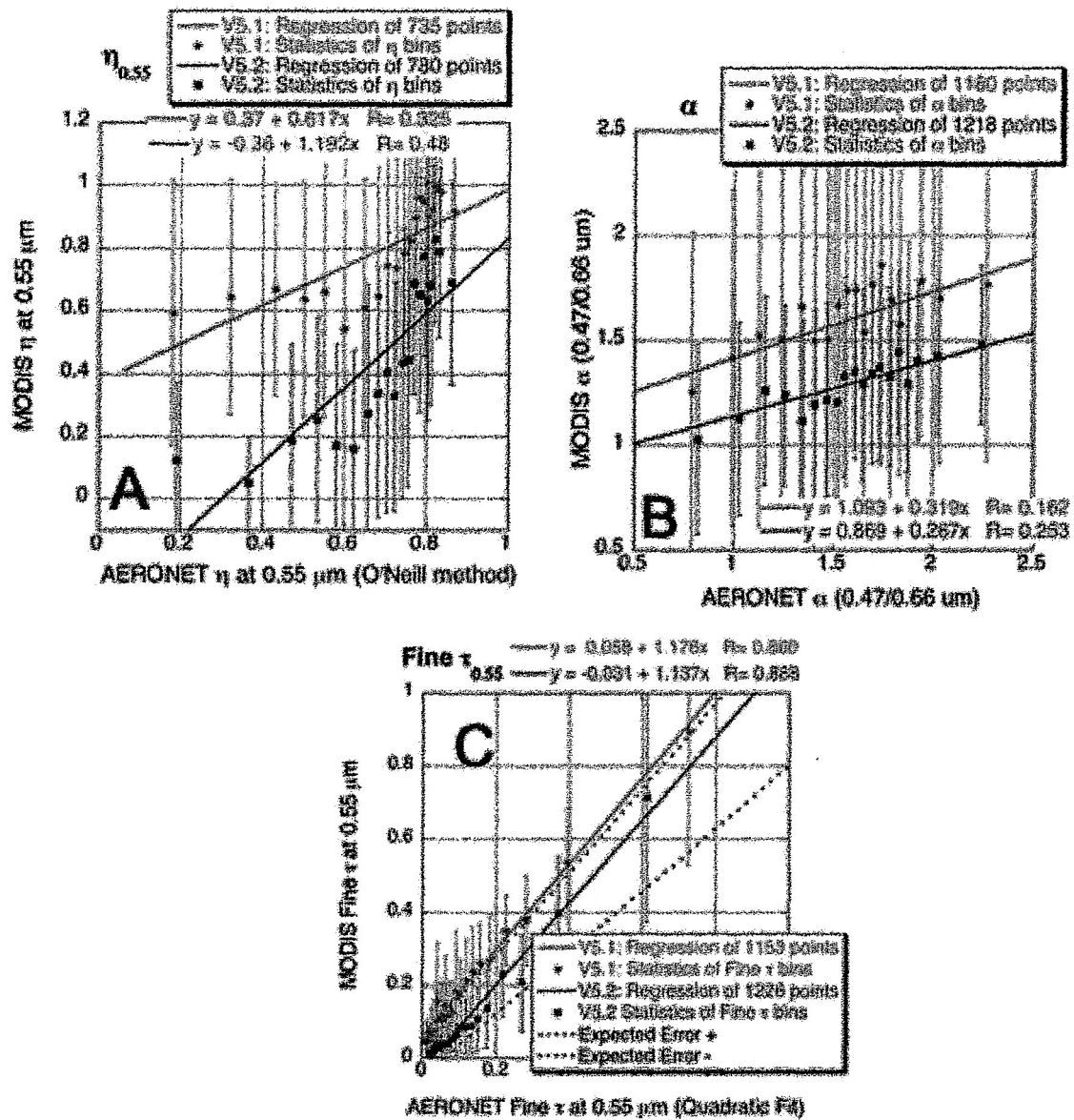
Figure 11: MODIS aerosol size retrievals compared with AERONET derived products. The solid shapes and error bars represent the mean and standard deviation of the MODIS retrievals, in 20 bins of AERONET-derived product. Both the retrievals from V5.1 (orange) and V5.2 (green) are shown. The regressions (solid lines) are for the cloud of all points (not shown). A) η over land retrieved at 0.55 μm, compared with AERONET η retrieved by the O'Neill method. Note that η is defined differently for MODIS and AERONET and that we only show results for τ > 0.20. B) MODIS-derived α (0.466/0.644 μm) over land with AERONET α interpolated to the same wavelengths. C) MODIS Fine τ over land retrieved at 0.55 μm, compared with AERONET Fine τ interpolated to 0.55 μm by quadratic fitting and the O'Neill method. The expected errors for MODIS ($\pm$0.05 $\pm$0.15τ) are also shown (dashed lines).